Understanding the Molecular Basis for FGF15/19 and FGF21 Actions on Energy Homeostasis

APPROVED BY SUPERVISORY COMMITTEE

Steven Kliewer, Ph.D.

David Mangelsdorf, Ph.D.

Melanie Cobb, Ph.D.

Makoto Kuro-o, M.D./Ph.D.

Joyce Repa, Ph.D.

To

My Husband, Jonathan, and My Parents, John & Peggy

Understanding the Molecular Basis for FGF15/19 and FGF21 Actions on Energy Homeostasis

by

JAMIE BONEY-MONTOYA

DISSERTATION

Presented to the Faculty of the Graduate School of Biomedical Sciences

The University of Texas Southwestern Medical Center at Dallas

In Partial Fulfillment of the Requirements

For the Degree of

DOCTOR OF PHILOSOPHY

The University of Texas Southwestern Medical Center at Dallas

Dallas, Texas

April, 2012

ACKNOWLEDGMENTS

Many people have contributed to my development and training during my time in science. I am grateful to my mentors, Drs. Steven Kliewer and David Mangelsdorf, for providing the opportunity to work in a wonderful laboratory. They offer outstanding resources and a creative scientific freedom that only a handful of labs are capable of providing. Steve and Davo have given me invaluable advice and support that has allowed me to pursue my scientific goals.

I would also like to express my deepest gratitude towards Matthew Potthoff. During my time as a graduate student, he has supported, encouraged, and mentored me. He has become an invaluable scientific resource as well as a great friend.

I am thankful to all the past and present members of the Mango/Kliewer lab for their time, help, and sharing of knowledge and reagents. In particular, I would like to thank Yuan Zhang, Xunshan Ding, Angie Bookout, and Vicky Lin for giving me mice, protocols, reagents, and teaching me new techniques. The Mango/Kliewer lab has been a great place to learn and a wonderful environment where I have made life-long friends.

I would like to thank my committee members, Drs. Melanie Cobb, Joyce Repa, and Makoto Kuro-o for their advice and time. I appreciate all of the feedback I received regarding my current work as well as my future plans.

I want to express my gratitude towards Ann Nardulli. I started my career in her lab at UIUC and I would not be here without her. She gave me a home and when I had to leave, she supported my decision. I could not have asked for a more understanding mentor.

I would also like to thank my parents, John and Peggy, for their love, support, and generosity. They have been a constant source of encouragement and inspiration. They are my heroes. I am also grateful to my brother, Johnathon, for reminding me that life is a gift and should be enjoyed.

Finally, I'd like to thank my husband, Jonathan, for his unwavering love and support. I recognize it can't be easy to live with someone who has western blots and journal articles scattered on our dining room table. I would especially like to thank him for never asking me when I would be finished with school. He has been my comfort and my strength throughout my tenure as a grad student. I would not be where I am without him.

I am especially appreciative to all my family and friends for giving me the balance I have needed for my happiness and success.

Understanding the Molecular Basis for FGF15/19 and FGF21 Actions on Energy Homeostasis

Jamie Boney-Montoya, Ph.D.

The University of Texas Southwestern Medical Center at Dallas, 2012

Supervising Professors: **Steven A. Kliewer, Ph.D & David J. Mangelsdorf, Ph.D.**

Insulin and glucagon have long been known to play essential roles in controlling energy balance during the fed and fasted states, respectively. Recently, additional metabolic hormones have been discovered within a subfamily of the fibroblast growth factor superfamily. The FGF15/19 subfamily is composed of atypical FGFs lacking the heparin-binding domain, which enables them to act in

an endocrine fashion by diffusing away from their tissues of origin. They signal through cell-surface receptors complexed with β-Klotho, a membrane-spanning protein, to mediate signaling cascades that lead to physiological responses. One member, FGF19, causes reduced glucose and insulin levels with enhanced insulin sensitivity when expressed in transgenic mice. Another member, FGF21, has been shown to act as an insulin sensitizer pharmacologically by improving glucose tolerance and reducing insulin. The prevalence of metabolic disorders (e.g. type 2 diabetes) in today's society has led to the investigation of these two endocrine FGFs for use in a clinical setting. However, the mechanisms underlying these responses have not been characterized.

To elucidate the mechanisms utilized by FGF15/19, we used several animal models to show a role for FGF15/19 in regulating hepatic glucose production. Like insulin, FGF15/19 represses gluconeogenesis. Specifically, FGF15/19 inhibits expression of the transcriptional coactivator PGC1α, a key regulator of gluconeogenic gene expression. The repressive effect of FGF15/19 on gluconeogenic gene expression is lost when PGC1α is overexpressed. FGF15/19 causes the dephosphorylation and inactivation of the transcription factor CREB, thereby blunting its ability to bind and induce the PGC1α promoter. The results demonstrated that FGF15/19 works subsequent to insulin as a postprandial regulator of gluconeogenesis through inhibition of the CREB/ PGC1α pathway.

To fully understand the effects of FGF21, we began studying the downstream kinase signaling cascades and the protein substrates affected by this hormone. Utilizing stable isotope labeling of amino acids in cell culture (SILAC), an unbiased phosphoproteomic profile was obtained of potential FGF21 targets in rat H4IIE hepatoma cells. One of the most highly regulated targets was FetuinA, which was dephosphorylated by FGF21 treatment. FetuinA is an inhibitor of insulin receptor signaling and the FetuinA knockout mouse exhibits aberrant glucose homeostatsis. Our *in vitro* data suggested a relationship between FGF21 and FetuinA in regulating insulin sensitivity but further exploration lead to the conclusion that FGF21 was not directly regulating FetuinA *in vivo.*

Taken together, the important role of FGF15/19 and FGF21 in regulating carbohydrate metabolism as well as their pharmacological actions makes them attractive drug candidates for metabolic diseases. However, further study will be required to determine their molecular mechanisms more completely and their long-term efficacy in the clinic.

Table of Contents

List of Publications

1. **Boney-Montoya J***, Potthoff MJ*, Choi M, Satapati S, He T, Suino-Powell K, Xu HE, Gerard RD, Finck BN, Burgess SC, Mangelsdorf DJ, Kliewer SA. (2011) FGF15/19 Regulates Hepatic Glucose Metabolism by Inhibiting the CREB-PGC1α Pathway. Cell Metab 13(6) 729-738. **** Equal Contributions***
2. **Boney-Montoya J**, Ziegler YS, Curtis CD, Montoya JA, and Nardulli AM. (2010) Long Range Transcriptional Control of Progesterone Receptor Gene Expression. Mol Endocrinol 24(2): 346-358.
3. Mao C, Patterson NM, Cherian MT, Aninye IO, Zhang C, **Montoya JB**, Cheng J, Putt KS, Herenrother PF, Wilson EM, Nardulli AM, Nordeen SK, Shapiro DJ. (2008) A new small molecule inhibitor of estrogen receptor alpha binding to estrogen response elements blocks estrogen-dependent growth of cancer cells. J Biol Chem 283 (19):12819-30.
4. Creekmore AL, Ziegler YS, **Boney JL**, Nardulli AM. (2007) Estrogen receptor alpha regulates expression of the breast cancer 1 associated ring domain 1 (BARD1) gene through intronic DNA sequence. Molecular and Cellular Endocrinology 267(1-2): 106-15.

List of Figures

List of Tables

List of Abbreviations

Ahsg	Alpha-2-HS-glycoprotein
BAT	Brown Adipose Tissue
CBP	CREB Binding Protein
CDC	Centers for Disease Control
ChIP	Chromatin Immunoprecipitation
CNS	Central Nervous System
CRE	cAMP Reponse Element
CREB	cAMP Regulatory Element Binding Protein
Cyp7A1	Cholesterol 7 alpha-Hydroxylase
DIO	Diet-Induced Obese
FGF	Fibroblast Growth Factor
FGF15/19	Fibroblast Growth Factor 15/19
FGF21	Fibroblast Growth Factor 21
FGFR	Fibroblast Growth Factor Receptor
FXR	Farnesoid X Receptor
G6Pase	Glucose 6-Phosphatase
GC/MS	Gas Chromatography/Mass Spectrometry
HBS	Heparin Binding Site
HFD	High-Fat Diet
HSGAG	Heparan Sulfate Glycosaminoglycans

I.P.	Intraperitoneal
IR	Insulin Receptor
ITT	Insulin Tolerance Test
KO	Knock Out
NMR	Nuclear Magnetic Resonance
PEPCK	Phosphoenolpyruvate Carboxykinase
PGC1α	Peroxisome Proliferator Activated Receptor gamma Coactivator 1-alpha
PKA	Protein Kinase A
PP1	Protein Phosphatase 1
PP2A	Protein Phosphatase 2A
PPARα	Peroxisome Proliferator Activated Receptor alpha
PPARγ	Peroxisome Proliferator Activated Receptor gamma
RT-qPCR	Real-Time quantitative PCR
SHP	Small Heterodimer Protein
Sub-Q	Subcutaneously
TCA	Tricarboxylic Acid Cycle
VDR	Vitamin D Receptor
WAT	White Adipose Tissue
WHO	World Health Organization

Chapter 1.

Background & Introduction

1.1 Overview

Insulin and glucagon have long been known to play essential roles in controlling energy balance during the fed and fasted states, respectively. Recently, additional metabolic hormones have been discovered within a subfamily of the fibroblast growth factor (FGF) superfamily. The FGF15/19 subfamily is composed of atypical FGFs lacking the heparin-binding domain, which enables them to act in an endocrine fashion by diffusing away from their tissues of origin (Goetz, Beenken et al. 2007). They signal through cell-surface receptors complexed with klotho family members, membrane-spanning proteins, to mediate signaling cascades that lead to physiological responses (Beenken and Mohammadi 2009). Pharmacologically, they have effects on glucose metabolism and insulin sensitivity (Tomlinson, Fu et al. 2002; Fu, John et al. 2004; Itoh and Ornitz 2004; Kharitonenkov, Shiyanova et al. 2005; Kharitonenkov, Wroblewski et al. 2007). This has led to the investigation of their use in a clinical setting for the treatment of metabolic disorders (e.g. type 2 diabetes).

I begin this introductory chapter with background on metabolic homeostasis and FGFs. I follow with a broad overview of the known physiology and pharmacology of FGF15/19 and FGF21. I also describe the prevalence of type 2 diabetes and obesity and how these endocrine FGFs can be utilized as prime drug candidates for use in the clinic. I conclude with the objectives of my

dissertation, as well as an outline of the studies I performed described in the subsequent chapters.

1.2 Metabolic Homeostasis

Energy homeostasis is the balance of energy input and output to maintain the body's nutritional needs. The regulation of metabolic homeostasis is mediated principally by hormonal and neural signals that lead to transcriptional, translational, and post-translational effects in various target tissues. In a normal physiological state, these signals coordinate responses to fluctuating energy availability. The primary source of energy is glucose, making it an important barometer of nutritional status. During high glucose levels (i.e. feeding), insulin is released from the pancreas to act on the muscle, liver, and white adipose tissue (WAT) to cause glucose uptake. In the muscle and liver, glucose is converted into glycogen. Insulin also acts on the liver to decrease de novo hepatic glucose production, gluconeogenesis. In the WAT, it converts glucose into fatty acids and inhibits lipolysis, the breakdown of lipids. Whereas in states of low glucose levels (i.e. fasting), glucagon is released from the pancreas into circulation where it acts on the liver to increase hepatic glucose output by increasing glycogenolysis, the breakdown of glycogen. Once liver glycogen stores have been depleted, triglycerides are broken down to provide substrates for gluconeogenesis and ketogenesis, the production of ketone bodies. Ketone bodies are utilized as an

alternate energy source when glucose levels are low. As fasting progresses into starvation, hepatic fatty acid oxidation is activated to provide additional energy sources. Although insulin and glucagon play critical roles in metabolic homeostasis, many other hormones have been identified as important regulators however their discussion is beyond the scope of this thesis.

1.3 Fibroblast Growth Factor Superfamily

The FGF superfamily is comprised of twenty-two distinct members and clustered into seven subfamilies based on phylogenetic analysis (Itoh and Ornitz 2004). FGFs are polypeptides that have been shown to play a multitude of roles (Itoh 2007; Itoh and Ornitz 2008). During embryonic development, they regulate morphogenesis, brain patterning, and limb development. In the adult organism, they are important for tissue repair, wound healing, angiogenesis, bile acid and energy homeostasis.

FGFs mediate their cellular responses by binding to and activating a family of cell surface receptor tyrosine kinases, the FGF receptors (FGFR), encoded by four genes (*Fgfr1-4*) (Beenken and Mohammadi 2009). The structural organization among the family of FGFRs is similar, each containing an extracellular ligand-binding domain with three immunoglobulin-like domains, a transmembrane domain, and the tyrosine kinase domain. The *Fgfr1-3* genes encode two splice variants within the immunoglobulin-like domain III, “b” and

"c", leading to differential ligand-binding preferences (Ornitz 2000; Mohammadi, Olsen et al. 2005). Most FGFs require an additional interaction with heparan sulfate glycosaminoglycans (HSGAG) in the extracellular matrix to activate the FGFR. HSGAGs protect FGFs against degradation, determine the distance FGFs can diffuse, and stabilize the protein-protein contacts between the FGF/FGFR interaction (Ornitz 2000). A FGF will simultaneously bind to the FGFR and HSGAG leading to receptor dimerization and autophosphorylation. The two main FGFR targets, PLCγ and FRS2α, are subsequently phosphorylated leading to the activation of the PI3K, MAPK, or STAT signaling pathways (Beenken and Mohammadi 2009). The induction of signaling cascades by FGFs results in the plethora of physiological responses.

The FGF superfamily can be categorized into three separate groups based on their mechanism of action; paracrine, intracrine, or endocrine factors. The functional divergence can be accounted for by key structural differences. FGFs typically contain the same homologous core region, a signal peptide sequence, and a heparin binding site (HBS). Paracrine FGFs, members of the FGF1, FGF4, FGF7, FGF8, and FGF9 subfamilies, are considered the classical FGFs that interact with both FGFRs and HSGAG (Ornitz 2000; Itoh and Ornitz 2008). The strong interaction between the HBS and HSGAG allows them to be sequestered within their tissue of origin. The intracrine FGFs (FGF11-14), also known as FGF homologous factors, lack the signal peptide sequence causing them to be localized

within the cell (Goldfarb 2005). Despite their high affinity for HSGAG and their high sequence identity to the FGFs, intracrine FGFs are unable to activate FGFRs. The endocrine FGFs, members of the FGF19 subfamily, have a weakened HBS enabling them to enter into the bloodstream and act on distant tissues. This makes them an unexpected and interesting addition to the growing list of hormones (Goetz, Beenken et al. 2007).

1.4 Endocrine Fibroblast Growth Factors

The endocrine FGFs are comprised of the three FGF19 subfamily members, FGF19, FGF21, and FGF23. FGF19, the human ortholog of the mouse FGF15, will be referred to as FGF15/19 unless it is specifically denoted as the mouse or human ortholog. Two key characteristics define the endocrine FGFs: their reduced HSGAG binding capacity and their gene expression regulation by nutrient sensing via nuclear hormone receptors.

Endocrine FGFs have a weakened HBS which allows them to diffuse away from their tissue of origin and limits the ability of HSGAG to promote the FGF/FGFR interaction (Goetz, Beenken et al. 2007). To overcome this limitation, endocrine FGFs require the presence of either α-Klotho or β-Klotho to elicit a signal (Kurosu and Kuro 2009). The Klotho family is comprised of three proteins, α-Klotho, β-Klotho, and lactase-like. All three are single-pass transmembrane proteins that can stabilize the endocrine FGF interaction with its cognate FGFR

(Kurosu, Ogawa et al. 2006; Kurosu, Choi et al. 2007; Fon Tacer, Bookout et al. 2010). Gene expression analysis of the Klotho family shows that α-Klotho is found most abundantly in the kidney, while β-Klotho is highly expressed in the liver, gallbladder, pancreas, white adipose tissue and brown adipose tissue (Fon Tacer, Bookout et al. 2010). Due to the restricted tissue distribution of the Klotho proteins, the target tissues of endocrine FGFs seem to be dictated by their presence. Extensive studies have shown that α-Klotho serves as the co-receptor for FGF23 (Kurosu, Ogawa et al. 2006), while β-Klotho is the co-receptor for both FGF15/19 and FGF21 (Kurosu, Choi et al. 2007).

The endocrine FGFs are the transcriptional targets of nuclear hormone receptors regulated by nutrient status. The nuclear receptor superfamily is comprised of 48 ligand-activated transcription factors (Mangelsdorf, Thummel et al. 1995). Subclasses of the nuclear receptor superfamily are activated by dietary lipids and vitamin availability, allowing nutritional status to regulate metabolic pathways. These metabolic receptors activate transcriptional programs that can control endocrine FGF expression (Moore 2007). In the case of FGF23, it is induced in the bone by activation of the Vitamin D Receptor (VDR) in response to high levels of vitamin D or high phosphate. FGF23 is then secreted where it can act on the kidney to regulate vitamin D and phosphate metabolism (Saito, Kusano et al. 2003; Larsson, Marsell et al. 2004). FGF15/19 and FGF21 are regulated during feeding and fasting, respectively. Feeding promotes the release

of bile acids from the gallbladder which can bind and activate the Farnesoid X Receptor (FXR), which induces the expression of FGF15/19 in the ileum. Secreted FGF15/19 acts on the liver to repress the expression of the Cyp7A1 gene, which encodes the rate limiting enzyme for bile acid synthesis (Holt, Luo et al. 2003; Inagaki, Choi et al. 2005). Fasting increases the release of fatty acids from white adipose tissue which can bind and activate the Peroxisome Proliferator-Activated Receptor α (PPARα), which induces the expression of FGF21 in the liver. Secreted FGF21 acts on the WAT, brown adipose tissue (BAT), and liver where it promotes expression of genes that regulate lipid and carbohydrate metabolism (Kharitonenkov, Shiyanova et al. 2005; Badman, Pissios et al. 2007; Inagaki, Dutchak et al. 2007; Lundasen, Hunt et al. 2007; Potthoff, Inagaki et al. 2009). The interesting roles endocrine FGFs play in physiology have led to further research into understanding their functions and mechanisms.

1.5 FGF15/19

FGF15 was originally discovered as a novel FGF found within the developing central nervous system (McWhirter, Goulding et al. 1997). It was later determined that FGF15 is the rodent ortholog of the human FGF19 (Nishimura, Utsunomiya et al. 1999). While most FGFs are highly conserved between rodents and humans, FGF15 and FGF19 only share roughly 50% amino acid identity.

Nevertheless, they are syntenic (Katoh 2003). FGF15 is expressed in the central nervous system (CNS) where it plays a role in neuronal differentiation during fetal development (McWhirter, Goulding et al. 1997; Gimeno, Brulet et al. 2003). In adulthood, FGF15 is no longer expressed in the CNS but is found very highly and specifically in the ileum of the small intestine (Fon Tacer, Bookout et al. 2010). The primary function of FGF15/19 in the adult is the regulation of bile acid homeostasis.

Bile acids are toxic and their concentrations must be tightly controlled. Postprandially, bile acids are released from the gallbladder into the small intestine where they emulsify lipids. They are reabsorbed once they reach the ileum where they are transported back to the liver or the gallbladder via the portal vein. The refilling of the gallbladder with bile is regulated by FGF15/19 (Choi, Moschetta et al. 2006). FGF15 KO mice have an empty gallbladder, even after fasting, that can be rescued with recombinant FGF19 treatment. Another function of bile acids, specifically cholic acid and chenodeoxycholic acid, is as ligands for the nuclear receptor, FXR (Kalaany and Mangelsdorf 2006). Once bound by bile acids, FXR inhibits the expression of cholesterol 7α-hydroxylase (Cyp7A1), the enzyme that catalyzes the rate-limiting step in the bile acid synthesis pathway (Russell and Setchell 1992). FXR mediates the repression of Cyp7A1 in the liver through two dependent mechanisms involving small heterodimer partner (SHP) and FGF15/19. SHP is an orphan nuclear receptor that lacks a DNA binding domain

but tethers to other nuclear receptors to elicit a transcriptional effect. SHP and FGF15/19 expression are induced by FXR activation in the liver and ileum, respectively (Goodwin, Jones et al. 2000; Lu, Makishima et al. 2000; Holt, Luo et al. 2003). SHP binds to the promoter of Cyp7A1, whereas FGF15/19 binds to the cell-surface FGFR4/β-Klotho complex to inhibit Cyp7A1 expression. Consistent with their function, both SHP KO and FGF15 KO mice have increased Cyp7A1 expression and bile acid pool sizes (Kerr, Saeki et al. 2002; Wang, Lee et al. 2002; Inagaki, Choi et al. 2005). Exogenous FGF15/19 treatment causes Cyp7A1 repression which is lost in the FGFR4 KO and β-Klotho KO mice (Yu, Wang et al. 2000; Inagaki, Choi et al. 2005; Ito, Fujimori et al. 2005; Tomiyama, Maeda et al. 2010). Interestingly, SHP is also required for FGF15/19 effects on Cyp7A1 (Inagaki, Choi et al. 2005). However, the detailed mechanism of Cyp7A1 repression by FGF15/19 is still under investigation.

Although bile acid homeostasis seems to be the main function of FGF15/19, the FGF19 transgenic mice suggested a possible role in glucose homeostasis. These mice had reduced glucose and insulin levels when compared to their wild-type (WT) counterparts. They displayed lower body weights and were resistant to high-fat diet (HFD) (Tomlinson, Fu et al. 2002). Similar metabolic phenotypes were also described in the leptin-deficient (Ob/Ob) mice treated with exogenous FGF19 (Fu, John et al. 2004). Taken together, these studies suggest a potential for FGF15/19 treatment in diabetic patients. However,

one major caveat is the development of hepatocellular carcinomas by the FGF19 transgenic mice (Nicholes, Guillet et al. 2002). Recently, the FGF19 polypeptide has been re-engineered to eliminate its proliferative capacity while maintaining its metabolic functions (Wu, Ge et al. 2010). This promising development has reignited an interest in using FGF15/19 as a treatment for type 2 diabetes.

1.6 FGF21

FGF21 was first identified as a novel FGF that was preferentially expressed in the adult mouse liver (Nishimura, Nakatake et al. 2000). However, the first description of its function was as a novel regulator of metabolic function (Kharitonenkov, Shiyanova et al. 2005). Researchers found that FGF21 administration lowered plasma glucose, insulin, and triglyceride levels and produced weight loss in diabetic mouse models. A FGF21 transgenic (FGF21tg) mouse model was also described to have improved glucose clearance and insulin sensitivity. This led to work in diabetic rhesus monkeys confirming the insulin-sensitizing effects. (Kharitonenkov, Wroblewski et al. 2007). These results led to a plethora of research to confirm the pharmacological effects of FGF21 (Coskun, Bina et al. 2008; Berglund, Li et al. 2009; Xu, Lloyd et al. 2009). However, a concern regarding its efficacy for clinical use became evident in a recent study revealing that FGF21 can significantly reduce bone mass (Wei, Dutchak et al. 2012).

Amidst these developments, several groups identified the physiological roles of FGF21 in the fasting and starvation response (Badman, Pissios et al. 2007; Inagaki, Dutchak et al. 2007; Lundasen, Hunt et al. 2007). During fasting and starvation, fatty acids are mobilized from the WAT to the liver where they are oxidized and used to synthesize ketone bodies. These ketone bodies are used as a primary fuel source, particularly by the brain, during periods when carbohydrates are not available. Another function of fatty acids is to act as ligands for the nuclear receptor, PPARα (Evans, Barish et al. 2004). Once bound by a fatty acid, PPARα, regulates the transcription of many genes involved in fatty acid transport and oxidation, including FGF21. PPARα KO mice develop hepatic steatosis and become hypoglycemic and hypoketonemic during fasting (Kersten, Seydoux et al. 1999; Leone, Weinheimer et al. 1999; Hashimoto, Cook et al. 2000). However, these effects could be partially rescued by administration of recombinant FGF21 (Inagaki, Dutchak et al. 2007). These experiments led to important discoveries in the roles of FGF21 in inducing torpor (Inagaki, Dutchak et al. 2007), inhibiting growth hormone (Inagaki, Lin et al. 2008), and promoting glucose and fatty acid catabolism (Potthoff, Inagaki et al. 2009). The regulation of these multiple metabolic pathways suggests several tissues are capable of responding to FGF21.

FGF21 requires the presence of β-Klotho and can function with FGFR1c, FGFR2c, or FGFR3c (Ogawa, Kurosu et al. 2007; Kharitonenkov, Dunbar et al. 2008; Suzuki, Uehara et al. 2008). The tissues exhibiting this expression profile

include the liver, WAT, BAT, hypothalamus, and pancreas (Fon Tacer, Bookout et al. 2010). The large number of FGF21-responsive tissues could explain the broad range of physiological and pharmacological effects.

1.7 Obesity & Type 2 Diabetes

The physiology of metabolic homeostasis is based on the premise that energy intake equals energy expenditure. A direct result of consuming more energy than is being expended is the accumulation of WAT and weight gain. The growing epidemic of obesity illustrates the ramifications of altering these finely tuned processes. According to the World Health Organization (WHO), overweight and obesity is the fifth leading risk of global death. Several serious conditions are associated with obesity, including insulin resistance and type 2 diabetes. Type 2 diabetes is a consequence of the body's inability to effectively secrete and/or utilize insulin resulting in hyperglycemia. Just as obesity rates are increasing, so are those of type 2 diabetes, with estimates of 346 million people affected in 2010 (WHO). The United States alone accounts for 25.6 million of these affected individuals with annual medical costs estimated at $174 billion (2007, CDC). Unfortunately, these numbers are growing at a rapid rate despite the several treatment options currently available. In response, research into the molecular basis of the diseases as well as new approaches for obesity and type 2 diabetes treatment are being investigated.

1.8 Aims

The role that FGF15/19 and FGF21 have in regulating glucose metabolism and insulin sensitivity pharmacologically has prompted an interest in elucidating the molecular mechanisms they utilize. Future use of these in the clinic requires a more thorough understanding of their physiological roles in mediating energy homeostasis and understanding the pathways they regulate to potentially mitigate side effects. My studies were designed to address these questions using two different approaches. In Chapter 2, I describe the materials and methods used throughout the course of my studies. In Chapter 3, I use several mouse models to delineate the role of FGF15/19 in regulating gluconeogenesis through a PGC-1α/CREB pathway. In Chapter 4, I used an *in vitro* system to define novel targets of FGF21. In Chapter 5, I summarize the conclusions of my dissertation and describe the broader implications of the data when examined together.

Chapter 2.

Materials & Methods

2.1 Animals & Animal Husbandry

All animal protocols were approved by the Institutional Animal Care and Research Advisory Committee at the University of Texas Southwestern Medical Center. FGF15 KO (C57BL/6;129S background), FGFR4 KO (C57BL/6;129S background), FGF21 KO (pure C57BL/6 background), FGF21tg (pure C57BL/6 background), total β-Klotho KO (C57BL/6;129S background), and liver-specific β-Klotho KO (C57BL/6;129S background) mice were all available in the Mangelsdorf/Kliewer laboratory. C57BL/6 mice were purchased from the mouse breeding core at the University of Texas Southwestern Medical Center. All animals were housed in a pathogen-free facility and maintained in a temperature-controlled environment with a 12-hour light/dark cycle. Animals had *ad libitum* access to water and irradiated rodent chow (TD.2916, Harlan-Teklad) unless otherwise specified. Diet-induced obese (DIO) mice were purchased from Jackson Laboratories, housed individually, and fed a 60% high-fat diet (D12492, Research Diets Inc). All experiments were performed using single-caged male mice. Mice were euthanized by carbon dioxide inhalation and exanguinated via the descending vena cava or decapitated. Tissues were collected, snap frozen in liquid nitrogen, and stored at -80°C until processed. Blood was collected in heparinized tubes (Sarstedt) and centrifuged at 5000rpm at 4°C for 30 minutes, aliquoted, snap frozen in liquid nitrogen, and stored at -80°C until processed.

2.2 Animal Procedures

Fasting experiments were performed from 6pm to 12am unless otherwise specified and 24 hour fasting experiments were performed from 9am to 9am. Overnight fasting experiments were performed from 6pm to 10am.

Oral glucose tolerance tests were performed on mice that were fasted overnight and given an oral glucose load of 2mg/g body weight. Tail vein blood was collected at the indicated time points.

Insulin tolerance tests were performed in mice that were fasted for 4-6 hours and given an intraperitoneal (I.P.) injection of 0.75U/kg body weight of insulin (Sigma-Aldrich). Tail vein blood was collected at the indicated time points.

Fasting-refeeding experiments were performed in mice that were fasted for 24 hours and given an oral bolus of 20ul/g body weight nutrient rich diet (Ensure, Abbott Laboratories). Tail vein blood was collected at the indicated time points.

For rhFGF21 injections, food was removed from the cage 1 hour prior to and during the treatment unless otherwise specified.

2.3 Adenovirus Infections

10–14 week old C57BL/6 males for FGF15 and PGC-1α overexpression studies or 12–14 week old PGC-1$\alpha^{fl/fl}$ mice for the Cre-recombinase experiment

were used. 7.5×10^9 particles/g body weight of adenovirus was delivered intravenously by jugular vein injection into mice. 3 days after infection of the control, FGF15, PGC-1α adenoviruses, or combination thereof, mice were administered 1ug/g body weight FGF19 or vehicle and fasted for the indicated time.

For acute, hepatic deletion of PGC-1α, Cre-expressing adenovirus or control adenovirus was administered to PGC-$1\alpha^{fl/fl}$ mice, followed by 9 days of recovery. Mice were then administered 1ug/g body weight FGF19 or vehicle and fasted for the indicated time.

7.5×10^9 particles/g body weight of an adenovirus expressing a cyclic AMP response element (CRE) driving luciferase (Ad-CRE-luc; a gift from Dr. Marc Montminy, Salk Institute) was injected by jugular vein into wild-type 12–16 week old C57BL/6 males. 3 days after infection, mice were administered vehicle or FGF19 and then fasted for 6 hours. Ad-CRE-luc activity was measured as described (Dentin, Liu et al. 2007). In vivo luciferase activity was measured using an IVIS lumina imaging system following luciferin injection, and luciferase activity (photons/second) was normalized to copies of virus DNA infected per liver determined by QPCR analysis of hexon gene expression (Hogg, Garcia et al. 2010).

2.4 *In Vivo* & *Ex Vivo* Tracer Studies

Livers were isolated and perfused for 60 minutes in a nonrecirculating fashion at 8 ml/min with a Krebs-Henseleit-based perfusion medium as described (Burgess, Weis et al. 2003). Oxygen consumption was determined by use of an oxygen electrode. Relative gluconeogenesis and glycogenolysis were determined using the deuterated water method with deuterium enrichment detected in effluent perfusate glucose by ^{2}H NMR. Relative fluxes through PC/PEPCK and the TCA cycle were determined using [U-$^{13}C_3$] proprionate as substrate and analyzing the effluent perfusate glucose by ^{13}C isotopomer analysis. Relative fluxes were multiplied by absolute hepatic glucose production to determine absolute flux through these pathways. Ketone and glucose production were determined from the effluent perfusate.

Pyruvate/lactate challenge experiments were performed by I.P. injection of 1g/kg body weight of uniformly labeled pyruvate ([U-$^{13}C_3$] pyruvate (sodium salt), Cambridge isotopes) and 2g/kg body weight of uniformly labeled sodium lactate ([U-$^{13}C_3$] lactate (sodium salt), Cambridge isotopes) into *ad libitum* fed mice at 8 pm. Pyruvate and lactate were provided together to minimize perturbations of redox state. 20 minutes prior to treatment, food was removed for the duration of the experiment. Tail vein blood was collected at the indicated times and plasma glucose analyzed. Remaining blood was used to measure

glucose enrichments by GC-MS (Sunny and Bequette 2010). M+3 was monitored and indicated conversion of pyruvate/lactate to glucose.

2.5 Hepatic Lipids

Liver lipids were extracted using the Folch method (Folch, Lees et al. 1957). 100 ug of liver tissue was homogenized in 2:1 chloroform/methanol, washed with 50 mM NaCl, and washed with 0.36 M CaCl2/Methanol. The organic phase was separated by centrifugation at 2000 rpm between washes and chloroform was added to a final volume of 5ml. 10ul of Triton-X 100/chloroform (1:1;v/v) was added to 100ul aliquots of each extract and dried under nitrogen. Colorimetric enzymatic assays were performed to measure cholesterol (Thermo Scientific) and triglycerides (Thermo Scientific) levels according to manufacturers' instructions.

2.6 Plasma Parameters

Total plasma cholesterol (Thermo Scientific), triglycerides (Thermo Scientific), glucose (Wako Chemicals), and ketones (Wako Chemicals) were measured using colorimetric assay kits according to manufacturers' instructions. Plasma insulin (Crystal Chem), FGF19 (Biovendor), and FGF21 (Biovendor) were analyzed using ELISA kits according to manufacturers' instructions. For

glucagon measurements, blood was collected, aprotonin was added immediately at 1000KIU/ml blood, and sent to the Vanderbilt Hormone Assay & Analytical Core (Vanderbilt University).

2.7 Cell Culture

Rat hepatoma cell line H411E, mouse hepatoma cell line Hepa1c1c6, and human hepatoma cell line HepG2, were purchased from the American Tissue Culture Collection (ATCC) and maintained in Dulbecco's modified Eagle's medium (DMEM), Alpha minimum essential medium (MEM) without ribonucleosides and deoxyribonucleosides, and Eagles' medium, respectively, each supplemented with 10% fetal bovine serum (FBS), 100U/ml penicillin G, and 100mg/ml streptomycin. Cell lines were incubated at 37 °C and 5% CO_2 and subcultured every 3-4 days. Prior to treatment, cells were incubated in serum-free media overnight unless otherwise stated. Cells were treated with vehicle, 100ng/ml rFGF19 or 1ug/ml rFGF21 unless otherwise stated.

One day before Stealth RNAi transfection, H4IIE cells were plated at a density of $5x10^5$ cells/well in 2ml of growth media without antibiotics in a 6-well plate format. 500pmol of either a Fetuin-A specific- or control- Stealth RNAi (Invitrogen) was diluted in 250ul of Opti-MEM Reduced Serum Medium (Invitrogen) and mixed. 5ul of Lipofectamine2000 (Invitrogen) was diluted in 250ul and incubated for 15minutes at room temperature. The Stealth RNAi and

Lipofectamine2000 were combined and incubated for 15minutes at room temperature to allow the complex to form. 500ul of mixture was added per well and cells were incubated for 6hours at 37 °C and 5% CO_2 before growth media was replaced. Cells were incubated 18hours before being treated with vehicle or 1ug/ml rFGF21 for the indicated times and harvested for either protein or RNA analysis.

2.8 Primary Hepatocytes

Human primary hepatocytes were obtained from the Liver Tissue Procurement and Distribution System as attached cells in six-cell plates in human hepatocyte maintenance media containing 100nM dexamethasone, 100nM insulin, 100U/ml penicillin G, and 100mg/ml streptomycin. Media was changed to serum-free Williams' E medium for overnight and then treated with vehicle or 100ng/ml FGF19 until harvested for protein or RNA isolation.

For isolation of rat primary hepatocytes, rats were anaesthetized and the liver isolated and perfused with wash buffer containing DMEM, 5% ssFBS, 10mM HEPES, 7.4, 100U/ml penicillin G, and 100mg/ml streptomycin. The rat liver was further perfused with digestion buffer containing 1xHBSS, 25mM HEPES, 7.4, BSA, Trypsin Inhibitor (Invitrogen), Type II Collagenase (Invitrogen), 100U/ml penicillin G, and 100mg/ml streptomycin. The digested rat liver was removed and placed into a petri dish containing plain DMEM. The

residual tissue was removed and the cells filtered through a cell strainer. The supernatant was removed and cells were washed, centrifuged at 93xg for 2 min, and resuspended in wash buffer. The viability of the cells was determined based on Trypan blue exclusion. Cells were resuspended in attachment medium containing Williams' E medium, 5% ssFBS, 100nM dexamethasone, 100nM insulin, 100U/ml penicillin G, and 100mg/ml streptomycin and plated in $1x10^6$ cells/well into 6-well plates. After 3 hours, attachment media was removed and serum-free experimental media containing DMEM, 100U/ml penicillin G, and 100mg/ml streptomycin was given. After an overnight incubation, cells were treated with 100ng/ml FGF19 or vehicle until harvested.

2.9 Stable Isotope Labeling of Amino Acids in Cell Culture

The following experiments were all done by the Merck Research Group and data was supplied to the Mango/Kliewer laboratory. Cell labeling for rat H4IIE cells was performed in heavy ($^{13}C_6$ Lys and $^{13}C_6$ Arg) and light ($^{12}C_6$ Lys and $^{12}C_6$ Arg) DMEM medium for five passages. The heavy or light Lys/Arg labeled cells were treated with vehicle or wild type FGF21 at 1 ug/ml (Ambrx) for 10 minutes. After the treatment, the cells were lysed and the protein concentrations of lysates were measured in five replicates. For lysates from both cell lines, equal amount of light and heavy $^{13}C_6$ Lys and $^{13}C_6$ Arg labeled lysates were mixed to generate the forward and reverse labeling samples. To examine the

quality of heavy isotope labeling and 1:1 mixing of heavy and light lysates, the forward and reverse labeling samples from both cell lines were analyzed by in-gel digestion with Trypsin followed by LC-MS profiling. Following mixing of cells and the subsequent proteolytic digestion with Trypsin and Endo-Protease LysC, immobilized metal affinity chromatography (IMAC-like) method was applied to enrich for phosphopeptides from both forward and reverse labeling samples prior to LC-MS analysis.

Fourier transform mass spectrometry (FTMS) was used to acquire high resolution mass spectrometry data from samples described above. Briefly, an aliquot of sample was loaded onto a micro-capillary liquid chromatography column. Peptides were bound and eluted from the column using a 120 minute HPLC solvent gradient. Eluted peptides were continuously converted to multiply charged peptide ions by electrospray ionization and introduced into the vacuum system of a LTQ-Orbitrap or LTQ-FT (Thermo-Fisher) mass spectrometer. High resolution mass spectra were acquired at a rate of 10 spectra per second. Tandem mass spectra were simultaneously acquired in a data dependent fashion and by targeted analysis of features of interest. These data were used to provide amino acid sequence information for selected peptide ions. Data files containing high resolution mass spectra and tandem mass spectra were acquired and uploaded to the Elucidator data analysis system (Rosetta Biosoftware).

Ion peak intensities from raw LC-MS/MS data files were analyzed by Elucidator PeakTeller algorithm to determine relative ratios of "light" to "heavy" peptide pairs (version 3.3). Raw MS/MS data were searched against the Merck rodent database using the SEQUEST or OMSSA algorithm.

2.10 RNA Purification & qRT-PCR

Total RNA was extracted using RNA STAT-60 (IsoTex Diagnostics) according to manufacturer's instructions. 2ug of RNA from each sample were DNAse treated and reverse transcribed using random hexamers. The resulting complementary DNA (cDNA) was analyzed by quantitative RT-PCR using methods described (Bookout, 2003). Relative mRNA levels were calculated using the comparative C_T method normalized to a housekeeping gene, either *cyclophilin* or *U36b4*. Primers were designed using Primer Express software (Applied Biosystems) and validated as previously described (Bookout, Jeong et al. 2006). The primer sequences used for gene expression analyses are listed in Table 2.1.

Table 2.1 RT-qPCR Primers

Genes	Orientation	Primer Sequence
m*Cyclophilin*	Forward Reverse	GGAGATGGCACAGGAGGAA GCCCGTAGTGCTTCAGCTT
r*Cyclophilin*	Forward Reverse	CCCTGAAGGATGTGATCATTG GGCAAAGGGTTTCTCCACTT
m*Cyp7A1*	Forward Reverse	AGCAACTAAACAACCTGCCAGTACTA GTCCGGATATTCAAGGATGCA

m*FetuinA*	Forward Reverse	CCACTTGCCATGCTTTGG CACCGCGTGCTCAGTCA
r*FetuinA*	Forward Reverse	GCTGGCAGAAAAGCAATATGG AACCTCTTCCCCACCAAGTC
m*G6Pase*	Forward Reverse	ACCTTGCGGCTCACTTTCC GAAAGTTTCAGCCACAGCAATG
m*Pepck*	Forward Reverse	CACCATCACCTCCTGGAAGA GGGTGCAGAATCTCGAGTTG
m*Pgc1α*	Forward Reverse	AGACAAATGTGCTTCCAAAAAGAA GAAGAGATAAAGTTGTTGGTTTGGC

m = mouse, r = rat

2.11 Phosphoprotein Purification

Phosphoproteins were isolated and purified from cells utilizing an affinity chromatography method using a phosphoprotein purification kit (Qiagen) according to manufacturers' instructions. Protein concentrations from all eluates were determined using the Lowry Assay (Pierce). Samples were diluted with 2X SDS sample buffer (Sigma) and boiled for 5 minutes and frozen at -20°C until processed.

2.12 Protein Isolation & Immunoprecipitation

Frozen livers were pulverized and ~100mg was homogenized in 500ul of liver lysis buffer containing 10mM Tris-HCl, pH 7.4, 5mM EDTA, 150mM NaCl, 10% Glycerol, 0.5% NP-40 with complete protease inhibitor cocktail (Roche) and phosphatase inhibitor cocktail (Roche). 100mg of frozen adipose tissue was

homogenized in 300ul of adipose lysis buffer containing 10mM Tris-HCl, pH 7.4, 5mM EDTA, 5mM EGTA, 150mM NaCl, 10% Glycerol, 1% NP-40, 0.5% Triton X-100, with complete protease inhibitor cocktail (Roche) and phosphatase inhibitor cocktail (Roche). Cells were collected with 300ul/well in a 6-well plate or 1ml/100mm plate of liver lysis buffer. Samples were centrifuged at 13000rpm for 30 minutes at 4°C and supernatants were collected. Plasma was depleted of albumin and IgG using the Proteome Purify 2 Immunodepletion Resin (R&D Systems) according to manufacturer's instructions. Protein concentrations from all supernatants were determined using the Lowry Assay (Pierce). Samples were diluted with 2X SDS sample buffer (Sigma), boiled for 3 minutes, and frozen at -20°C until processed.

For immunoprecipitations, supernatants were incubated with either IgG (Santa Cruz) or Fetuin-A antibody (Santa Cruz) at 1:50 dilution and pulled down with Protein G beads (Millipore) overnight at 4°C on an end-over-end tube rotator. Immunoprecipitants were washed 4X with 500ul lysis buffer and centrifuged for 2 minutes at 300 x g at 4°C to pellet beads. The beads were boiled with 2X SDS sample buffer (Sigma) for 3 minutes and eluate was collected by centrifuging and transferred to a clean tube.

2.13 Immunoblot Analysis

30-50ug of lysates or immunoprecipitants were resolved on a 10% SDS-polyacrylamide gel and transferred to a nitrocellulose membrane (Bio-Rad). The membrane was blocked in 5% milk/TBS-T and probed with a specific antibody at 4°C overnight followed by a secondary horseradish peroxidase-conjugated antibody. Proteins were resolved by either Enhanced Chemiluminescense (ECL) western blotting substrate (Pierce) or SuperSignal WestFemto chemiluminescense substrate (Pierce) according to manufacturers' instructions. Membranes were stripped and reprobed with antibody against β-actin (Sigma-Aldrich) as a loading control. Primary antibodies were prepared in a 3% BSA/TBS-T solution and secondary antibodies in a 5% milk/TBS-T solution. The antibody dilutions used for western blotting are listed in Table 2.2.

Table 2.2 Western Blot Antibody Dilutions

Antibody	Supplier	Dilution
β-Actin (AC-15)	Sigma Aldrich	1:10000
p-AKT (Ser473)	Cell Signal	1:1000
Total AKT	Cell Signal	1:1000
p-CREB (Ser133)	Montminy Lab	1:2000
Total CREB (48H2)	Cell Signal	1:1000
p-ERK1/2 (Thr202/Tyr204)	Cell Signal	1:1000
Total ERK1/2 (137F5)	Cell Signal	1:1000
pSer309 FetuinA	Mango/Kliewer Lab	1:200
Pan-FetuinA	Mango/Kliewer Lab	1:500
Rat FetuinA (Clone 774761)	R & D Systems	1:1000
Mouse Total-FetuinA (C-17)	Santa Cruz	1:1000
p-FOXO1 (Ser256)	Cell Signal	1:1000
Total FOXO1 (C29H4)	Cell Signal	1:1000

p-FRS2α (Tyr436)	Cell Signal	1:500
p-PRAS40 (Thr246)	Cell Signal	1:2000
Total PRAS40 (D23C7)	Cell Signal	1:1000
PGC1α (H-300)	Santa Cruz	1:1000
Phospho–Ser/Thr PKA Substrate	Cell Signal	1:1000
PP2A, Catalytic unit (1D6)	Millipore	1:1000
Rabbit anti-Goat IgG HRP	BioRad	1:1000
Goat anti-Rabbit IgG HRP	BioRad	1:5000
Goat anti-Mouse IgG HRP	BioRad	1:2000

2. 14 Chromatin Immunoprecipitation

300mg of liver from each sample of four mice were pulverized and pooled. Each pool was fixed in 1%formaldehyde/PBS for 10 minutes and quenched with 5M glycine for 5 minutes. Samples were dounce homogenized in a hypotonic buffer (10mM HEPES, pH 7.9, 1.5mM MgCl2, 10mM KCl, 0.2%NP-40, 1mM EDTA, 1% Sucrose) and layered over cushion buffer (10mM Tris-HCl, pH 7.5, 15mM NaCl, 60mM KCl, 1mM EDTA, 10% Sucrose) followed by centrifugation at 200 x g. Crude nuclear extracts were isolated and chromatin was isolated using the ChIP EZ Kit (Upstate) according to manufacturer's instructions. 3ug of protein from the sonicated chromatin was used for each immunoprecipation with either rabbit IgG (Cell Signal), anti-AcH3 (Upstate), anti-CREB (Cell Signal), anti-CBP (Santa Cruz), or anti-PGC-1α (Santa Cruz). Primers scanning the promoter region of the PGC-1α, G6Pase, and PEPCK genes from +500 to -3500 were designed and used for qPCR as described (Bookout,

Jeong et al. 2006). Primer sequences used for analyzing promoter occupancy are listed in Table 2.3.

Table 2.3 ChIP qPCR Primers for Mouse gDNA

Genes	Location	Orientation	Primer Sequence
m*PGC1α*	CRE −211/−146	Forward Reverse	CAGAGGGCTGCCTTGGA CAGCCTCCCTTCTCCTGTG
m*G6Pase*	CRE −179/−110	Forward Reverse	TGTGCCTGTTTTGCTATTTTACG AAGGTGCATCATCAGTAGGTTGA
m*G6Pase*	+600	Forward Reverse	CAACGACCTTGAATTGCTCAA CTAAACTACACGTGGGAACACACA
m*G6Pase*	+235	Forward Reverse	TCTTAAAGAGACTGTGGGCATCA TCACCCCTCGGGATGGT
m*G6Pase*	-250	Forward Reverse	CAGCCTCTAGCACTGTCAAGCA GCCATTGGCAGAGCCAAT
m*G6Pase*	-640	Forward Reverse	GACCATCCAGTGCTCTTAACCA TTATACTTCTTAGGGCAAGAAAACAATC
m*G6Pase*	-1000	Forward Reverse	GAACGTTCTCCACGACTTTAGG CGGAGAGTGTTTGTAATTCACTTG
m*G6Pase*	-1880	Forward Reverse	GGCATGACTGTGGTCCAACAC CCAATTTACTCTGTTCAAAAGGATATCC
m*G6Pase*	-2300	Forward Reverse	GCTGGTCATTGCATCCACTTT AGGGACAGACCAAAAACCTCACT
m*G6Pase*	-2730	Forward Reverse	TGTCTCTTCTGGTGAGACACATTC ACACGGTGGCCAGTATCCTA
m*G6Pase*	-3250	Forward Reverse	CGTTTTGTACCAAGAGACTAGGA AGCCTGTTGGGAAACTGACA
m*G6Pase*	-3875	Forward Reverse	GGAGTTCCCGGCAGTTGT CCCACAGAGGACCCATGTT
m*Pepck*	CRE −162/−96	Forward Reverse	CCCTGGAGTTTATTGTGTTAAGTCAGT GCAGGCCTTTGGATCATAGC
m*Pepck*	+860	Forward Reverse	TCAGTTGGCTGGCTCTCACT TGACTGTCTTGCTTTCGATCCT
m*Pepck*	+230	Forward Reverse	TGGGTGCTCCATGGTGTT GAACTCTGGTGCCACCTGAA
m*Pepck*	-200	Forward Reverse	CATTCATTAACAACCACAAGTTCAA CAGCACGGTTTGGAACTGA
m*Pepck*	-665	Forward Reverse	TGTCCTGTCAGAACAAAGCTTACA TCTCTGGCCATCCCAAGAT
m*Pepck*	-950	Forward Reverse	CCAGACACTTGGGCATTCAA AGTTCTGCGTTAGACACCATCAC

m*Pepck*	-1670	Forward Reverse	CAGCTGAATTAATAGTCTCTCCTTTTTT TGCCGTTTGTTTCAACTTAACC
m*Pepck*	-2105	Forward Reverse	GCAGCTGGCAACCAACAC CTTCCTACTGCTTCATCTTGAAGAA
m*Pepck*	-2360	Forward Reverse	TGGCCTTCCTCTCTTCCTCTTT TGGCTTTCTGTCAAGTCTGTAAACA
m*Pepck*	-3380	Forward Reverse	TGGGAGACACACATCTTATTCCA GGTGTGGCCCAGATTAAAGG
m*Pepck*	-3950	Forward Reverse	TGAGTGAACGCATGTGATTCC TCGTCATTGTCTTCTCCAATTTAGA

2.15 Antibody Production & Purification

Peptide design was based on the phosphorylation sites found on Fetuin-A determined by the SILAC experiments described in Section 2.9. The peptide sequences are located in Table 2.4. All peptides were synthesized and purified by the Protein Chemistry Technology Center at UT Southwestern Medical Center. Each peptide was crosslinked with keyhole limpet hemacyanin (KLH, Calbiochem) and m-Maleimodobenzoic acid N-hydroxysuccinimide ester (MBS, Sigma) for 1hour with stirring at room temperature. Two rabbits were immunized per peptide and injected 3x with 100ug crosslinked peptide in Freund's Adjuvant Complete (Sigma) once and Freund's Adjuvant Incomplete (Sigma) every 2 weeks after. All injections were administered subcutaneously (Sub-Q). Each rabbit was bled to obtain 30ml of blood before immunization, 5x after the first boost once per week, and exanguinated for the final bleed by the Animal Resource Center at the University of Texas Southwestern Medical Center.

For affinity purification columns, 1mg of peptide was immobilized to agarose using the SulfoLink Immoblization Kit for Peptides (Pierce) per manufacturers' instructions. Each antibody was purified first using a cognate phosphorylated peptide affinity column as positive selection and second a cognate non-phosphorylated peptide affinity column as negative selection. For affinity column purification, the column was equilibrated and the sample was applied to the column in 1x TBS. The column was incubated with rocking at room temperature for 1 hour before allowing the sample to flow through and elute. Column was allowed to elute and the sample collected. Column was washed 3x with 1xTBS. The bound protein was eluted 3x with 2ml of 0.1M Glycine, pH 3 into a tube containing 100ul of 1M Tris-HCl, pH 8.5. All samples and eluates were evaluated for the presence of antibody using western blot analysis. Specificity and phospho-specificity of the antibodies were tested using the pre-immune serum and peptide blocking as controls in western blot analysis. Phospho-specificity was also tested in plasma samples that had been treated with Lambda Protein Phosphatase (New England Biosciences) per the manufacturers' instructions and analyzed with western blot.

Table 2.4 FetuinA Antibody Immunizing Peptides

Antibody Target	Immunizing Peptide
Serine 134	HSTPDS*AEDVRKLC
Serine 309	HAFSPVAS*VESASGETLHSC
Serine 314	HAFSPVASVESAS*GETLHSC
Serine309/314	HAFSPVAS*VESAS*GETLHSC

* denotes phosphoryated amino acid

2.16 Statistical Analysis

Data are presented as mean ± standard error of the mean (SEM) and were analyzed by two-tailed, unpaired Student's t-test using the GraphPad Prism 5 software suite.

Chapter 3.

FGF15/19 Regulates Glucose Metabolism by Inhibiting the CREB-PGC1α Pathway

3.1 Introduction

FGF15/19 is a postprandial hormone that is induced in the ileum by bile acids from the gallbladder acting through the nuclear receptor, FXR (Inagaki, Choi et al. 2005). FGF15/19 acts to repress bile acid synthesis in liver and promote gallbladder filling (Holt, Luo et al. 2003; Inagaki, Choi et al. 2005; Choi, Moschetta et al. 2006; Lundasen, Galman et al. 2006). Plasma FGF19 levels peak 2–3 hr after a meal in humans (Lundasen, Galman et al. 2006). Transgenic mice expressing FGF19 in muscle have a higher basal metabolic rate and are resistant to high-fat-diet-induced weight gain (Tomlinson, Fu et al. 2002). These mice also have lower serum glucose and insulin levels and enhanced insulin sensitivity. Similar results were seen in Ob/Ob mice treated with exogenous FGF19 (Fu, John et al. 2004). These experiments suggest a role for FGF15/19 in glucose metabolism.

cAMP regulatory element-binding protein (CREB) is a transcription factor that regulates liver metabolism in response to fasting. The activity of CREB is determined by its phosphorylation status mediated through a diverse range of extracellular signals (Mayr and Montminy 2001). An example is glucagon through its action on protein kinase A (PKA), which phosphorylates CREB at Ser133 causing an activation of multiple transcriptional programs (Dalle, Longuet et al. 2004). The phosphorylation of CREB enables it to interact with coactivator

proteins, such as CREB-binding protein (CBP), to elicit a transcriptional response (Chrivia, Kwok et al. 1993; Kwok, Lundblad et al. 1994).

One particular gene induced by CREB during fasting is peroxisome proliferator-activated receptor γ coactivator protein-1α (PGC-1α) (Herzig, Long et al. 2001). PGC-1α encodes a coactivator protein that interacts with several transcription factors to induce the expression of genes involved in gluconeogenesis, fatty acid oxidation, tricarboxylic acid (TCA) cycle flux, and mitochondrial oxidative phosphorylation (Puigserver and Spiegelman 2003; Burgess, Leone et al. 2006; Finck and Kelly 2006; Handschin and Spiegelman 2006). PGC-1α overexpression has been shown to restore gluconeogenic gene expression and glucose homeostasis in CREB-deficient mice (Herzig, Hedrick et al. 2003).

In this chapter, I show a novel role for FGF15/19 in regulating hepatic glucose production. Like insulin, FGF15/19 represses gluconeogenesis. The results demonstrate that FGF15/19 works subsequent to insulin as a postprandial regulator of gluconeogenesis through inhibition of the CREB/ PGC-1α pathway.

3.2 Results

Although FGF15/19 had been postulated to be involved in energy homeostasis, the physiological relevance had yet to be determined. We set out to examine the role of FGF15/19 in glucose metabolism using a fasting/refeeding

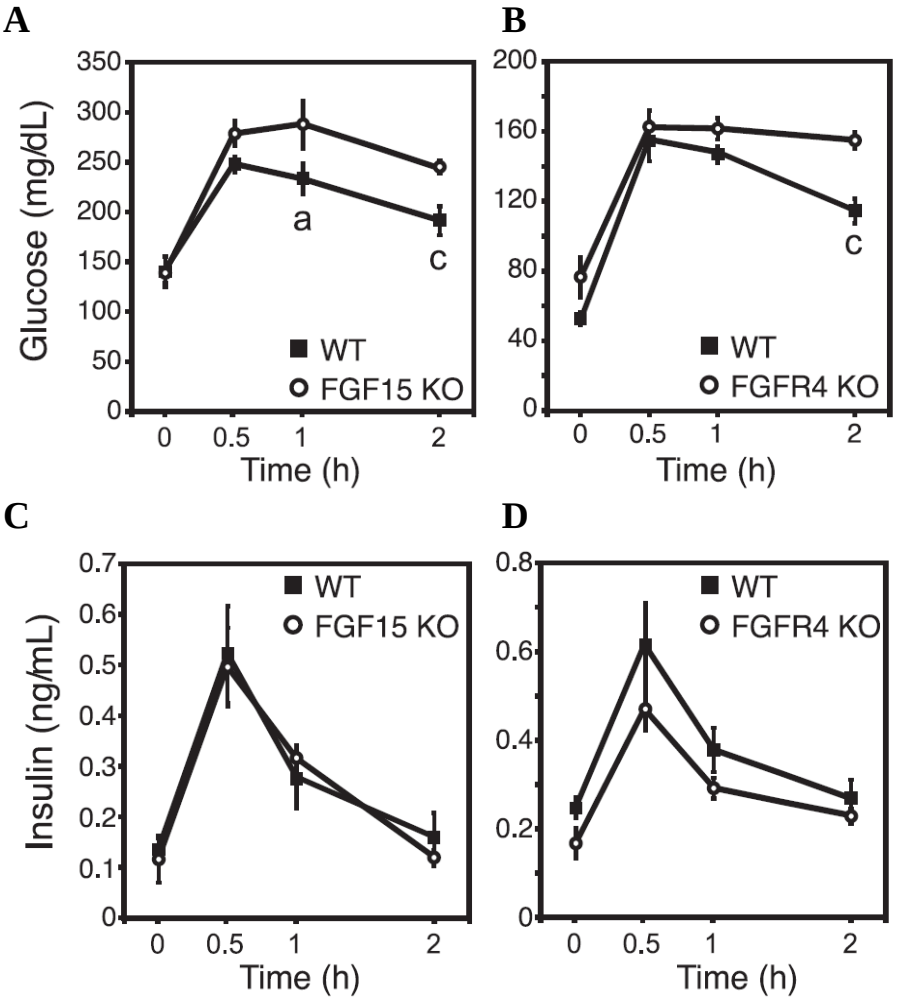

Figure 3.1: FGF15/FGFR4 Axis is Required to Maintain Normal Glucose Production

FGF15 KO mice, FGFR4 KO mice, and their WT counterparts were orally gavaged a bolus dose of nutrient rich liquid diet (n=6/group) following a 24h fast. Tail vein blood was collected intermittently. Plasma (A&B) glucose and (C&D) insulin levels were measured. Data are presented as mean ± SEM (a, $p < 0.05$; and c, $p < 0.005$).

paradigm in the FGF15 KO and FGFR4 KO mouse models. Animals from both genotypes and their wild-type (WT) counterparts were fasted for 24hr, fed a high carbohydrate/high fat liquid diet by oral gavage, and their blood glucose levels were analyzed over time. Blood glucose levels were elevated significantly in the FGF15 KO mice at the 1 and 2 hr time points (Fig. 3.1A) and in the FGFR4 KO mice at the 2 hr time point (Fig. 3.1B), indicating an impaired postprandial response when the FGF15-FGFR4 pathway is disrupted. Plasma insulin levels were not altered in either FGF15 KO or FGFR4 KO mice although there was a trend toward decreased plasma insulin concentrations in the FGFR4 KO mice (Fig. 3.1 C & D). These data demonstrate the contribution of the FGF15/FGFR4 axis to maintain normal glucose production.

Dr. Matthew Potthoff performed complimentary experiments to determine if FGF15/19 was regulating other liver metabolic functions utilizing metabolic flux by $^{2}H/^{13}C$ nuclear magnetic resonance (NMR) isotopomer analysis in perfused livers isolated from mice infected with either FGF15-expressing or control adenoviruses. The adenoviral expression of FGF15 significantly reduced hepatic gluconeogenesis, TCA cycle flux and β-oxidation and ketogenesis trended lower (Fig. 3.2B). In experiments performed in parallel, adenoviral expression of FGF15 decreased plasma glucose concentrations and caused downward trends in insulin but did not alter plasma glucagon concentrations (Fig. 3.2A). Taken

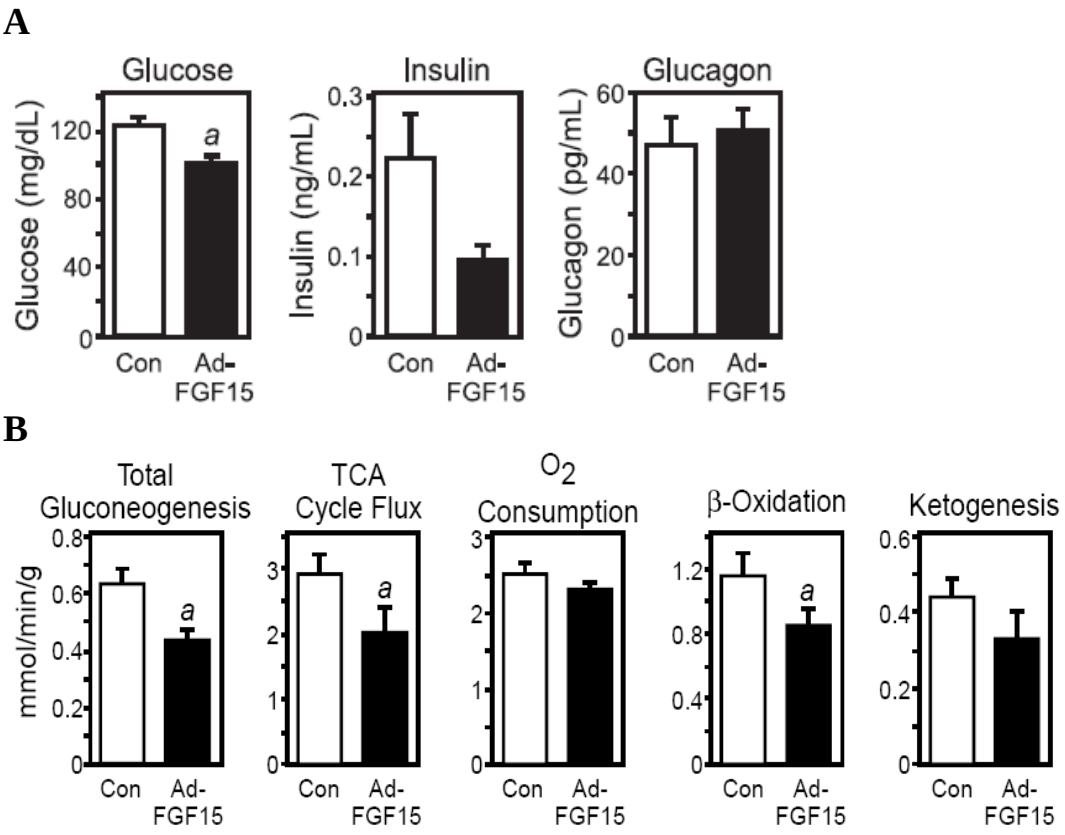

Figure 3.2: FGF15 Reduces Hepatic Gluconeogenesis, TCA Cycle Flux, and β-Oxidation

WT mice were infected with either control or FGF15 adenovirus for 3d (n=8/group). (A) Plasma parameters were measured from mice fasted 6hr. (B) Metabolic pathway flux measured by NMR from perfused livers of mice fasted overnight. Data are presented as mean ± SEM (a, $p < 0.05$).

together, these NMR isotopomer and metabolic parameter data demonstrate that FGF15/19 suppresses several hepatic metabolic pathways, including gluconeogenesis, TCA cycle flux and fatty acid oxidation, which are induced during fasting.

To directly assess the physiologic relevance of the FGF15/19 pathway in regulating gluconeogenesis, we performed a modified pyruvate/lactate challenge using uniformly labeled ^{13}C pyruvate and lactate in fed wild-type and FGF15-KO mice. I.P. administration of pyruvate/lactate caused a significantly greater increase in plasma glucose levels in FGF15-KO mice compared to wild-type mice (Fig. 3.3A). Mass spectrometry analysis verified that the additional plasma glucose was derived from labeled substrate (Fig. 3.3B). Taken together, these data demonstrate that FGF15 contributes to the repression of gluconeogenesis in the fed state.

To determine whether FGF15/19-mediated repression of gluconeogenesis might be the result of increased insulin sensitivity, insulin tolerance tests (ITT) were performed in FGF15 KO and FGFR4 KO mice and revealed no changes in insulin sensitivity (Fig. 3.4A & B). In addition, ITTs were performed in mice administered either vehicle or FGF19, or mice administered control or FGF15-expressing adenovirus. In these experiments, mice treated with FGF19 or FGF15 exhibited similar insulin sensitivity compared to their respective controls (Fig.

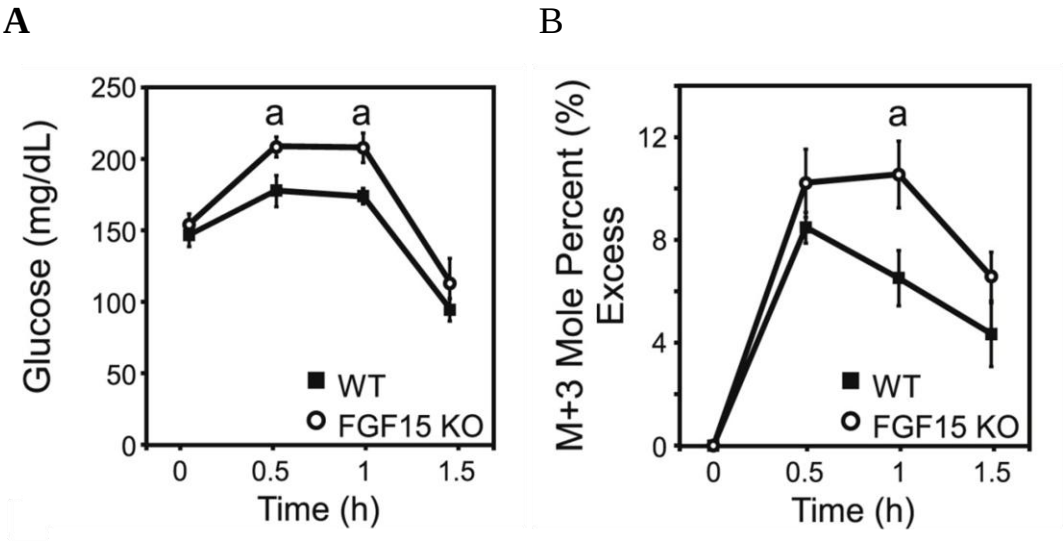

Figure 3.3: FGF15 Contributes to the Repression of Gluconeogenesis
Fed WT and FGF15 KO mice were I.P. injected with labeled pyruvate and sodium lactate (n=5-6/group). Tail vein blood was collected intermittently. Plasma (A) glucose levels and (B) mole percent (%) labeled glucose vs. unlabeled glucose was measured. Data are presented as mean ± SEM (a, $p < 0.05$).

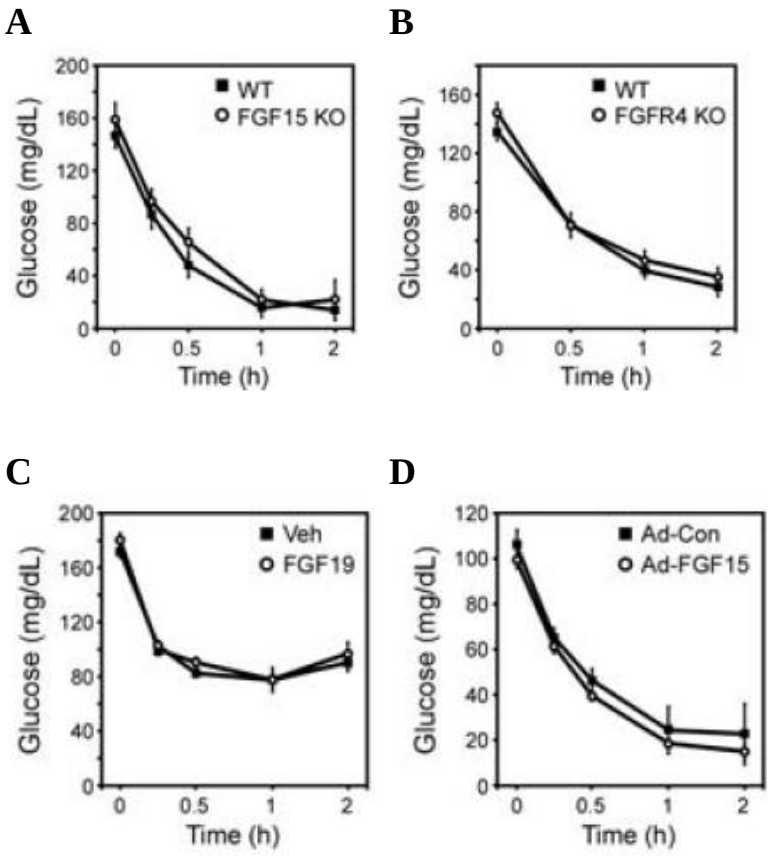

Figure 3.4: The FGF15/FGFR4 Axis Has No Effect on Insulin Sensitivity
(A) FGF15 KO or (B) FGFR4 KO and their WT counterparts were subjected to insulin tolerance tests (ITT). WT mice were (B) treated with vehicle or 1.0mg/kg FGF19 (n=6/group) or (C) infected with either control or FGF15 adenovirus for 3d (n=6/group) before being subjected to an ITT. Tail vein blood was collected intermittently to measure plasma glucose levels. Data are presented as mean ± SEM.

3.4°C & D). Thus, the FGF15-FGFR4 pathway modulates postprandial carbohydrate homeostasis without affecting insulin sensitivity.

A previous experiment done by Dr. Matthew Potthoff to determine the *in vivo* actions of FGF15/19 utilizing microarray analysis for livers from fasted wild-type mice treated with either vehicle, FGF15 or FGF19 for 6 hr was used as a reference. As expected, FGF15 and FGF19 both suppressed mRNA expression of the bile acid synthesizing enzyme, *Cyp7A1* (Fig. 3.5A) (Holt et al., 2003; Inagaki et al., 2005). Interestingly, one of the most strongly down-regulated genes in FGF15/19 treated livers was *Pgc1α* (Fig. 3.5A). There were corresponding decreases in PGC1α protein (Fig. 3.5B) and the PGC1α target genes glucose-6-phosphatase (*G6Pase*) and phosphoenolpyruvate carboxykinase (*Pepck*) which encode proteins involved in gluconeogenesis (Fig. 3.5A). As expected, *Pgc1α*, *G6pase*, *Pepck*, and *Cyp7A1* were significantly reduced in liver from mice administered Ad-FGF15 (Fig. 3.5C). To determine the kinetics with which FGF19 regulates gene expression, wild-type mice were fasted overnight to induce gluconeogenesis, administered FGF19 and then sacrificed over a 6 hr time course. *Cyp7A1* mRNA levels were reduced within 4 hr of FGF19 treatment (Fig. 3.5D). Likewise, *Pgc1α*, *Pepck*, and *G6pase* mRNAs were significantly reduced at the 4 and 6 hr time points (Fig. 3.5D). These results demonstrate that FGF15/19 regulates the expression of genes involved in gluconeogenesis. To assess the contribution of the FGF15/FGFR4 axis in regulating gluconeogenic gene

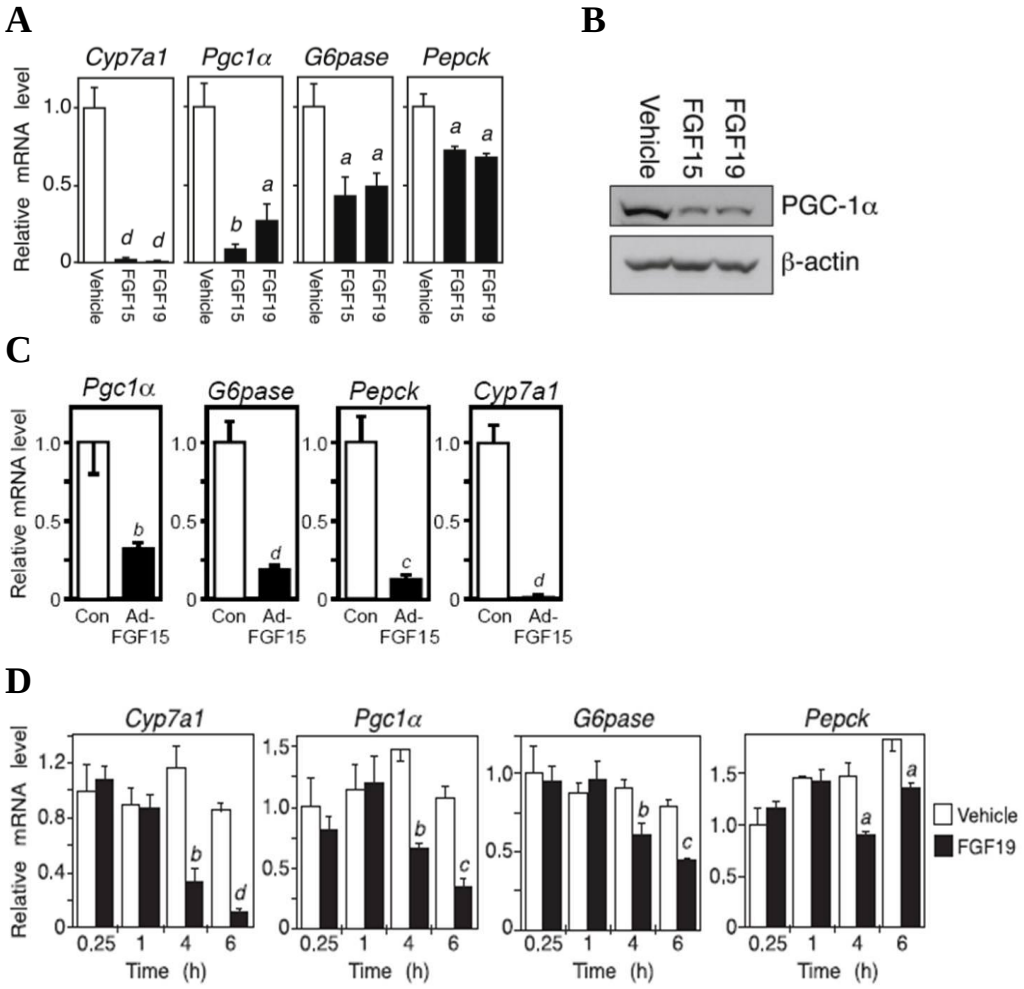

Figure 3.5: FGF15/19 Represses PGC1α and Gluconeogenic Gene Expression (A & B) WT mice were I.V. injected with vehicle, 0.15 mg/kg FGF15, or 1.0 mg/kg FGF19 for 6h (n=4/group) and fasted during the treatment period. (C) WT mice were I.P. injected with vehicle or 1.0mg/kg FGF19 for 6hr (n=4/group) after overnight fast. (D) WT mice were infected with either control or FGF15 adenovirus for 3d (n=5/group) and fasted overnight. (A, C, & D) Hepatic mRNA was measured by qPCR. Data are represented as the mean ± SEM (a, $p < 0.05$; b, $p < 0.01$; c, $p < 0.005$; and d, $p < 0.001$). (B) Liver homogenates were pooled and subjected to Western blot analysis.

expression, fed FGF15 KO and FGFR4 KO mice were examined. *Pgc1α*, *Pepck* and *G6pase* mRNA levels were significantly elevated in livers from fed FGF15 KO and FGFR4 KO mice (Fig. 3.6). Thus, the FGF15/FGFR4 axis is required to maintain *Pgc1α* and gluconeogenic gene expression.

We next used loss-of-function and gain-of-function studies to determine whether PGC-1α is required for FGF15/19-mediated repression of gluconeogenic gene expression. For loss-of-function studies, floxed PGC-1α mice (PGC-1α$^{fl/fl}$) (Lin, Wu et al. 2004) were administered either control adenovirus (Ad-Con) or a Cre recombinase-expressing adenovirus (Ad-Cre) to eliminate PGC-1α in liver. Groups of PGC-1α$^{fl/fl}$;Ad-Con and PGC-1α$^{fl/fl}$;Ad-Cre mice were subsequently fasted and administered either vehicle or FGF19. PGC-1α$^{fl/fl}$;Ad-Cre mice had the expected reduction in *Pgc1α* mRNA in liver and also had reduced basal expression of *G6Pase* and *Pepck* (Fig. 3.7A). As expected, FGF19 repressed expression of *Pgc1α*, *G6pase*, *Pepck* and *Cyp7A1* in PGC-1α$^{fl/fl}$;Ad-Con mice. However, the repressive effect of FGF19 on *G6pase* and *Pepck* was lost in PGC-1α$^{fl/fl}$;Ad-Cre mice (Fig. 3.7A) but not of *Cyp7A1*. Thus, FGF19-mediated repression of PGC-1α is important for the regulation of genes involved in carbohydrate metabolism but not bile acid metabolism. In complementary gain-of-function studies, wild-type mice were infected with either Ad-Con or a PGC-1α-expressing adenovirus (Ad-PGC-1α). Ad-PGC-1α caused a 15- to 20-fold increase in hepatic *Pgc1α* mRNA but did not further increase basal *G6pase* and

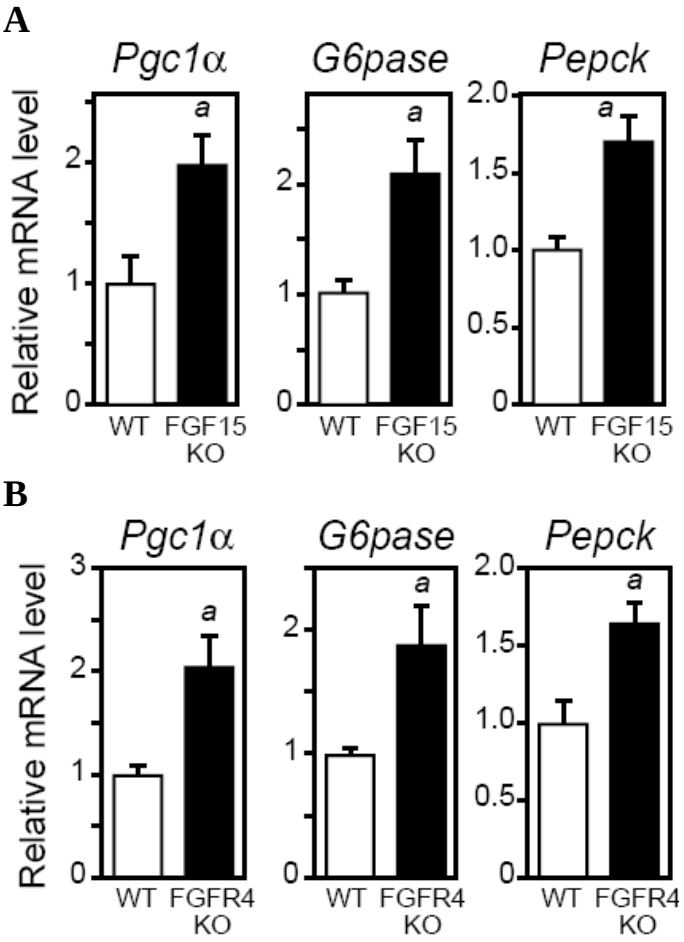

Figure 3.6: The FGF15/FGFR4 Axis is Required to Maintain PGC1α and Gluconeogenic Gene Expression

Hepatic mRNA was measured by qPCR from fed (A) FGF15 KO mice, (B) FGFR4 KO mice, and their WT counterparts. Data are represented as mean ± SEM (a, $p < 0.05$).

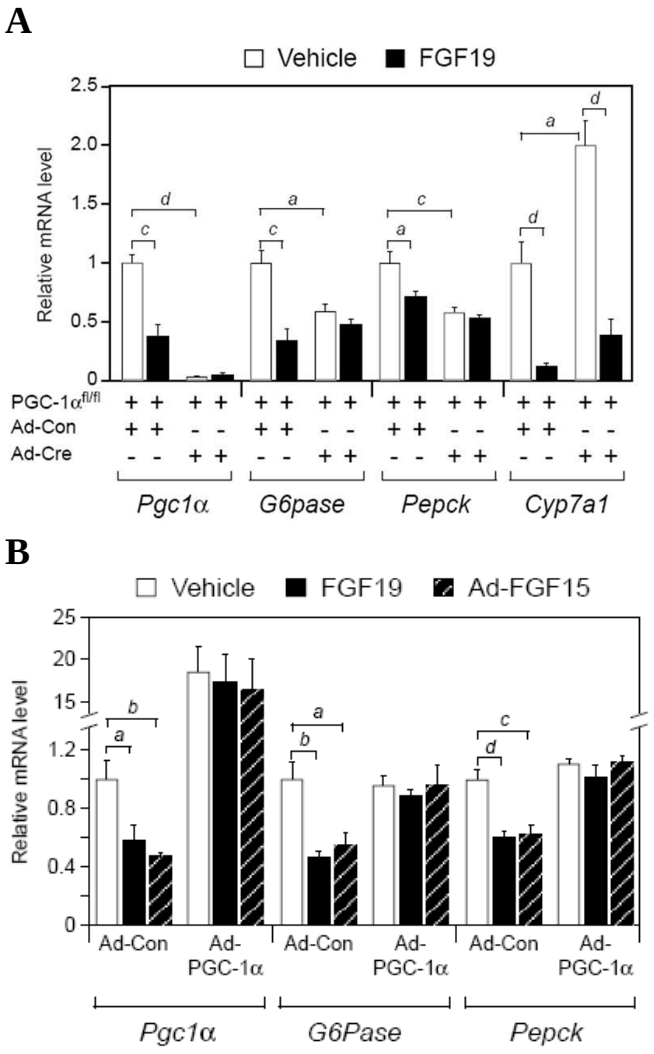

Figure 3.7: PGC1α is Required for FGF15/19 Repression of Gluconeogenic Gene Expression

(A) PGC1α fl/fl mice were infected with control or Cre-expressing adenovirus for 9d (n=5-6/group). (B) WT mice were infected with control or PGC1α-expressing adenovirus for 3d and a subgroup were coadministered a FGF15-expressing adenovirus (n=5-7/group). (A & B) Mice were treated with either vehicle or 1.0mg/kg FGF19 for 6hr and fasted during the treatment period. Hepatic mRNA was measured by qPCR Data are expressed as the fold change ± SEM (a, $p < 0.05$; b, $p < 0.01$; c, $p < 0.005$; and d, $p < 0.001$).

Pepck expression under these fasted conditions (Fig. 3.7B). Subgroups of these mice were either infected with an FGF15-expressing adenovirus (Ad-FGF15) or administered FGF19. As expected, FGF15 and FGF19 repressed *Pgc1α*, *G6pase* and *Pepck* in Ad-Con mice (Fig. 3.7B). However, under conditions of PGC-1α overexpression, neither FGF15 nor FGF19 repressed *G6pase* or *Pepck* (Fig. 3.7B). Taken together, the loss-of-function and gain-of-function data demonstrate that the effects of FGF15/19 on metabolic gene expression are mediated via regulation of PGC-1α.

To gain insight into how FGF15/19 represses *Pgc1α*, we analyzed candidate signaling pathways for activation by FGF19 *in vivo*. The CREB and FOXO1 phosphorylation cascades were chosen based on their characterized response elements within the *Pgc1α* promoter (Fig. 3.8A). Fasted wild-type and FGFR4-KO mice were administered FGF19 or vehicle for 30 min. As expected, administration of FGF19 increased FRS2α and ERK1/2 phosphorylation in liver of wild-type but not FGFR4-KO mice (Fig. 3.8B). FGF19 had no effect on the phosphorylation of either Akt or FOXO1. However, FGF19 caused a marked reduction in the phosphorylation of CREB at Ser133, a site that regulates CREB transcriptional activity (Gonzalez and Montminy 1989), in wild-type but not FGFR4-KO mice (Fig. 3.8B).

A

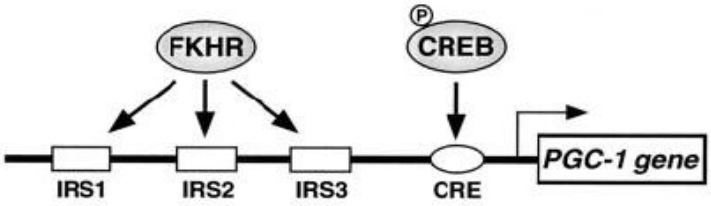

B

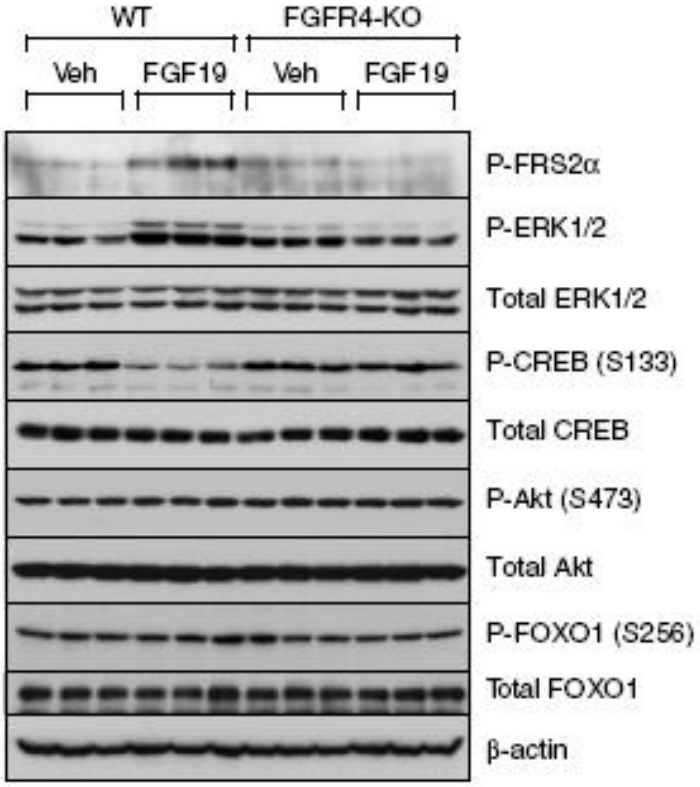

Figure 3.8: FGF19 Regulates CREB Phosphorylation Status
(A) Simplified diagram of FOXO1 and CREB response elements in the PGC1α promoter. Adapted from Daiko et al. (B) WT or FGFR4 KO mice were injected with either vehicle or 1.0mg/kg FGF19 for 30min (n=3/group) following an overnight fast. Liver lysates were subjected to Western blot analysis.

Since CREB induces *Pgc1α* by binding to a cAMP response element (CRE) in the *Pgc1α* promoter and recruiting coactivator proteins such as CBP (Herzig, Long et al. 2001), we performed chromatin immunoprecipitation (ChIP) analysis for CREB and CBP using liver from mice treated with vehicle or FGF19. We were unable to detect phosphorylated CREB due to technical reasons but CBP recruitment can be used a surrogate. Administration of FGF19 reduced CREB and CBP binding to the *Pgc1α* promoter (Fig. 3.9B). CREB and CBP binding were also reduced in liver from mice infected with an FGF15-expressing adenovirus (Fig. 3.9A). These data indicate that FGF15/19 inhibits *Pgc1α* expression by reducing the phosphorylation and transcriptional activity of CREB. Additional ChIP analyses of the *G6Pase* and *Pepck* promoters showed that FGF15 also reduced PGC1α binding to these promoters (Fig. 3.10). Interestingly, FGF15 decreased CREB binding to the *G6Pase* promoter but not the *Pepck* promoter (Fig. 3.10). Supplementary analyses of the *G6Pase* and *Pepck* promoters revealed several differences between the two. The *G6Pase* promoter has defined regions of active chromatin where CREB and PGC1α are bound (Fig. 3.11A, C, & E), whereas the *Pepck* promoter does not have a cohesive binding pattern of CREB and PGC1α (Fig3.11 D & F) or chromatin structure (Fig. 3.11B)

To confirm the effect of FGF15/19 on hepatic CREB activity, wild-type mice were infected with an adenovirus containing a CRE-luciferase reporter (Ad-

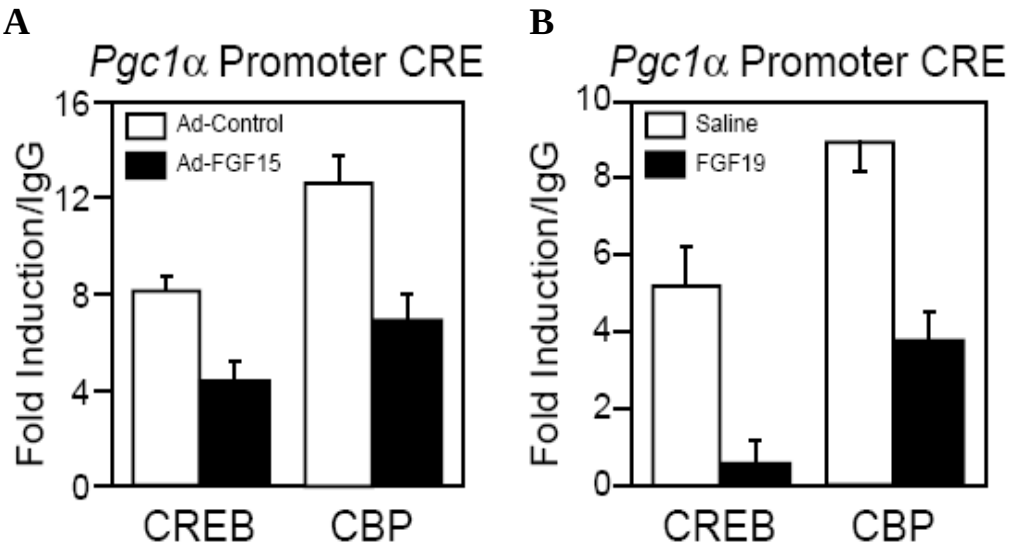

Figure 3.9: FGF15/19 Reduces CREB & CBP Binding to the *PGC1α* Promoter

(A) WT mice were treated with vehicle or 1mg/kg FGF19 for 1h (n=4/group) and fasted during treatment period. (B) WT mice were infected with control or FGF15 adenovirus for 3d (n=4/group) and fasted for 24h. ChIP assays were performed in pooled liver homogenates using an IgG control, CREB, CBP, or PGC1α specific antibody. DNA was isolated and subjected to qPCR. Data shown are expressed as fold change over IgG ± SEM.

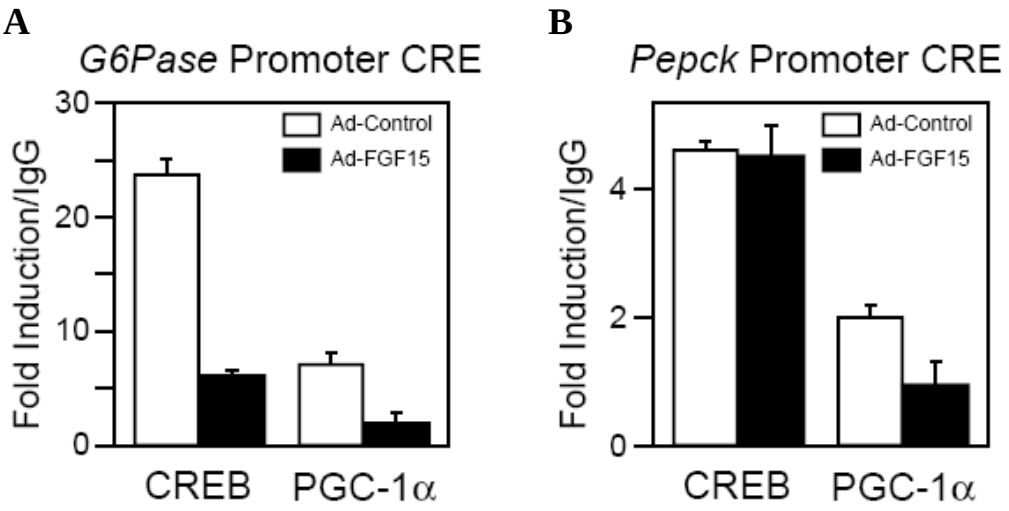

Figure 3.10: FGF15 Reduces PGC1α Binding to the *G6Pase* and *PEPCK* Promoters

WT mice were infected with control or FGF15 adenovirus for 3d (n=4/group) and fasted for 24h. ChIP assays were performed in pooled liver homogenates using an IgG control, CREB, or PGC1α specific antibody. DNA was isolated and subjected to qPCR at the (A) G6Pase or (B) PEPCK Promoter. Data shown are expressed as fold change over IgG ± SEM.

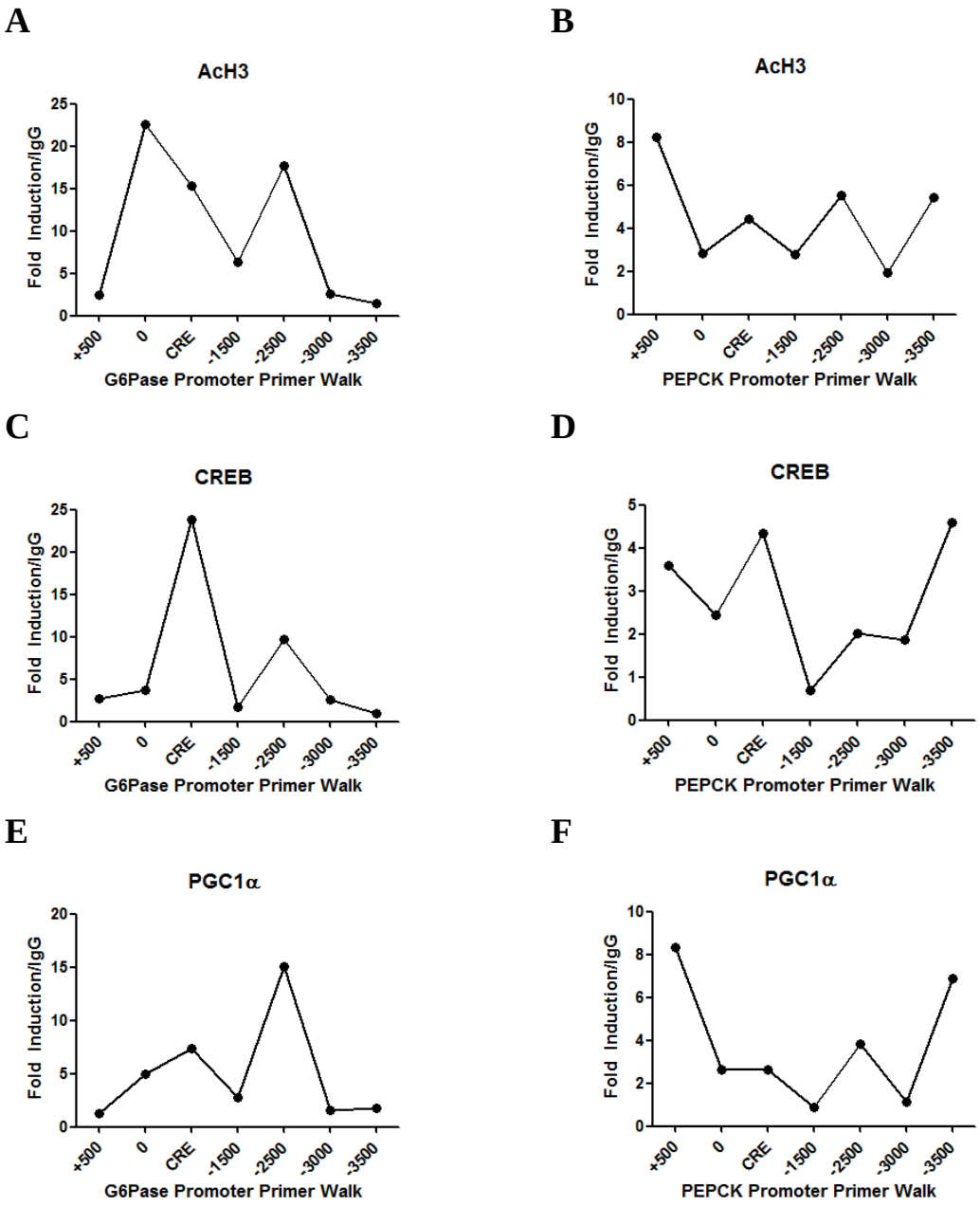

Figure 3.11: *G6Pase* and *PEPCK* Promoter Analysis in Fasted Mice
ChIP assays were performed in pooled liver homogenates from WT mice fasted for 24h using an IgG control, AcH3, CREB, or PGC1α specific antibody. DNA was isolated and subjected to qPCR. Data shown are expressed as fold change over IgG.

CREluc) (Wang, Vera et al. 2009) and then administered either vehicle or FGF19. As expected, Ad-CRE-luc-infected mice treated with vehicle showed significant induction of luciferase activity in response to a 6 hr fast (Fig. 3.12). This induction of luciferase activity was markedly attenuated in mice treated with FGF19 (Fig. 3.12). Thus, FGF19 efficiently suppresses hepatic CREB activity *in vivo*.

To elucidate the mechanism of the decrease in CREB phosphorylation and activity, we explored several possibilities. The rapidity with which CREB is dephosphorylated in liver suggests that FGF15/19 might activate phosphatases. Several CREB phosphatases, including PP1 and PP2A, have been described (Hagiwara, Alberts et al. 1992; Wadzinski, Wheat et al. 1993). However, PP1 and PP2A activity in liver extracts prepared from mice treated with FGF19 for 30min were unchanged (Fig. 3.13). Next, we examined whether CREB is a substrate of PKA in liver extracts from FGF19 treated mice. However, we did not detect changes in PKA activity by western blot analysis using a phosphorylated PKA substrate antibody (Fig. 3.14). Additionally, we sought to utilize various cell culture systems to determine the mechanisms involved. However, we were unable to detect differences in CREB phosphorylation in the presence of FGF19 treatment in all in vitro systems tested (Fig. 3.15, data not shown) Thus, additional studies will be required to determine how FGF15/19 affects CREB phosphorylation.

A

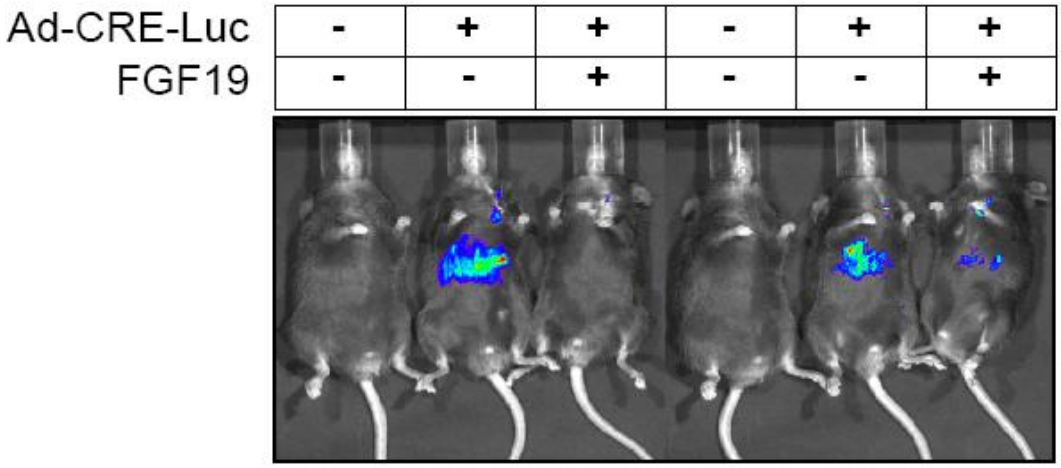

B

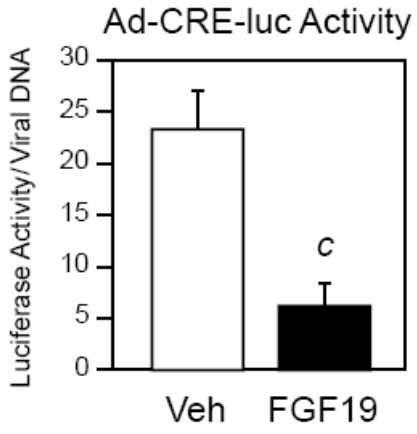

Figure 3.12: FGF19 Reduces CREB Activity *in vivo*
WT mice were infected with CRE-containing luciferase reporter adenovirus for 4d (n=6/group), treated with vehicle or 1.0mg/kg FGF19 for 6h and fasted during treatment period. (A) Mice were imaged for luciferase activity. (B) Quantified luciferase activity was normalized to the number of virus particles per liver. Data are represented as mean ± SEM (c, $p < 0.005$).

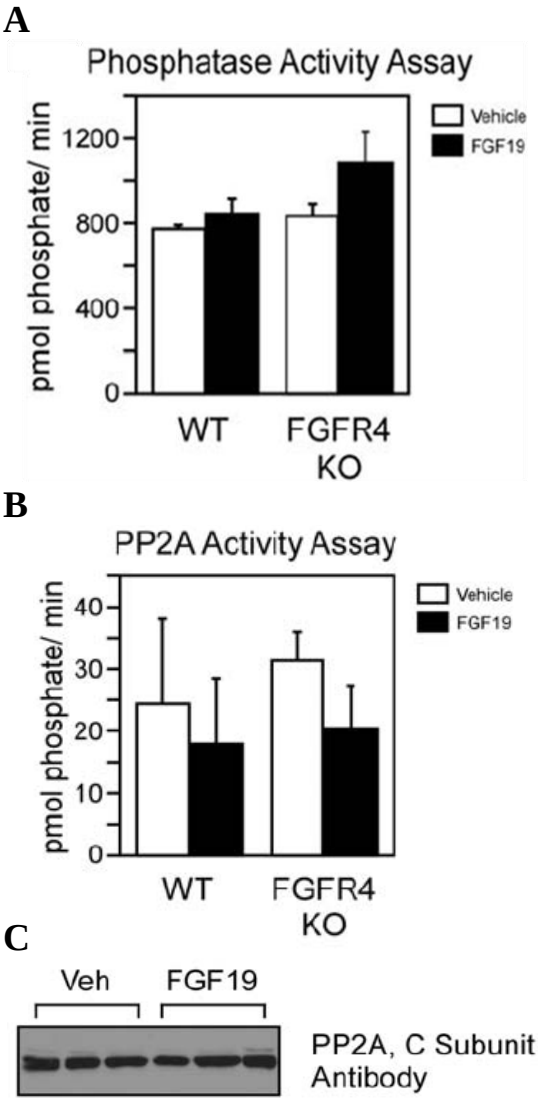

Figure 3.13: Hepatic Phosphatase Activity is Unchanged by FGF19 Treatment

WT or FGFR4 KO mice were injected with either vehicle or 1.0mg/kg FGF19 for 30min (n=3/group) following an overnight fast. Total hepatic (A) PP1/PP2A activity and (B) PP2A activity was measured and data are represented as mean ± SEM. (C) Liver lysates were subjected to Western blot analysis.

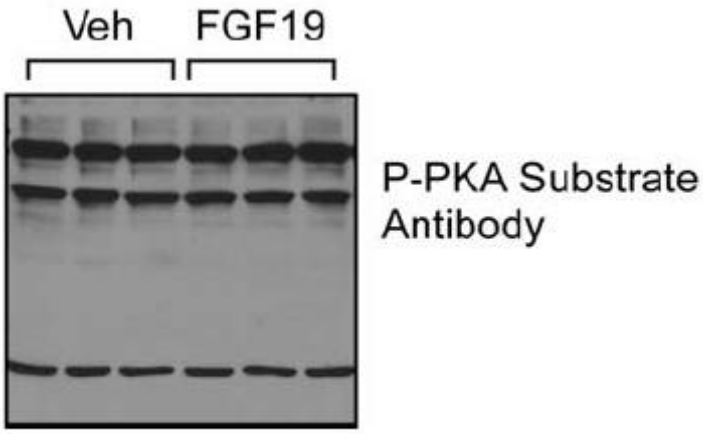

Figure 3.14: Hepatic PKA Activity is Unchanged by FGF19 Treatment
WT mice were injected with either vehicle or 1.0mg/kg FGF19 for 30min (n=3/group) following an overnight fast. Liver lysates were subjected to Western blot analysis.

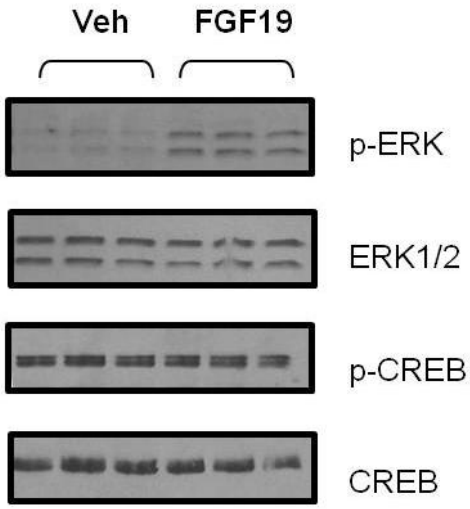

Figure 3.15: CREB Phosphorylation is Unaffected by FGF19 *in vitro*
HepG2 cells were treated with either vehicle or 1.0ug/ml FGF19 for 30min. Lysates were prepared and subjected to Western blot analysis.

We next examined the relative timing of FGF15 and insulin action in a physiological context. Wild-type mice were fasted for 24 hr and then gavaged with a high carbohydrate/high fat liquid diet. Plasma insulin (Fig. 1D) and glucose levels (Fig. 1E) peaked sharply within 15 min after refeeding as did liver levels of phosphorylated Akt (Fig. 1F), a measure of insulin action. For technical reasons we are unable to directly measure circulating FGF15 concentrations. As surrogates, we measured *Fgf15* mRNA in ileum and phosphorylation of ERK1/2 in liver, which is stimulated by FGF15/19 (Kurosu, Choi et al. 2007). *Fgf15* mRNA levels increased gradually in the ileum, peaking around 1 hr post-gavage (Fig. 1D). ERK1/2 phosphorylation in liver showed a very similar profile (Fig. 1F). These data suggest that postprandial FGF15 levels and signaling activity peak after those of insulin and are consistent with serum FGF19 concentrations in humans peaking 2–3 hr following a meal, well after insulin levels decrease (Lundasen, Galman et al. 2006). Plasma glucagon concentrations decreased only modestly after refeeding (Fig. 1E), which is not surprising given that glucagon levels are already low following a 24 hr fast(Ahren and Havel 1999; Parker, Andrews et al. 2002). CREB phosphorylation was reduced within 15 min of refeeding, remained relatively low at the 30 and 60 min time points and then increased (Fig. 1F), suggesting that both insulin and FGF15 suppress CREB activity.

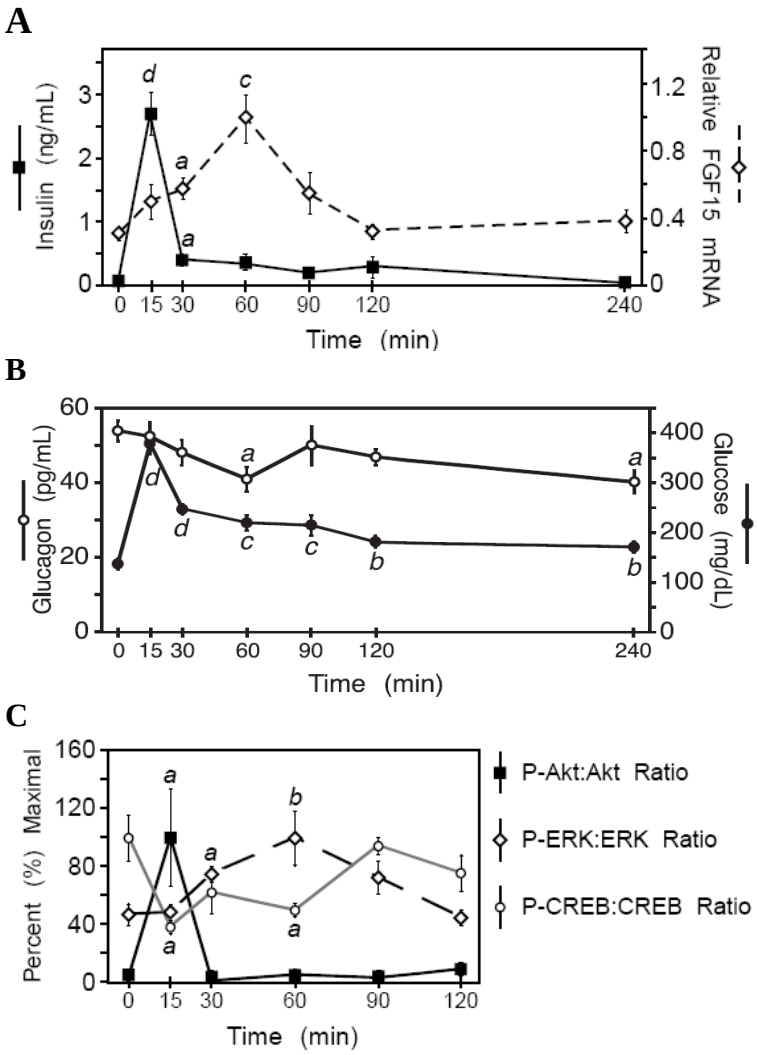

Figure 3.16: Postprandial Induction of Feeding Signals in the Mouse
WT mice were orally gavaged a bolus dose of nutrient rich liquid diet (n=5/group) following a 24h fast. Plasma (A) insulin, (B) glucose, and (B) glucagon levels were measured and presented as mean ± SEM. (A) Ileal mRNA was measured using qPCR. Data are expressed as the fold change ± SEM. (C) Liver lysates were subjected to Western blot analysis with phosphorylated and total antibodies. Quantification of hepatic phosphorylated protein was normalized to total protein. Data are expressed as percent of maximal phosphorylation ± SEM for each protein. (a, $p < 0.05$; b, $p < 0.01$; c, $p < 0.005$; and d, $p < 0.001$).

3.3 Discussion

In this series of experiments, we show that FGF15/19 plays a role in regulating hepatic glucose production. Like insulin, FGF15/19 represses hepatic gluconeogenesis. Recently, our lab also showed that FGF15/19 stimulates glycogen and protein synthesis in liver (Kir, Beddow et al. 2011). The striking overlap in the actions of FGF15/19 and insulin on liver highlighted the importance in understanding the temporal and mechanistic differences. Insulin is released rapidly from the pancreas following a meal. In our fasting-refeeding experiments, serum insulin concentrations and downstream Akt phosphorylation in liver peaked approximately 15 min after gavage with a high carbohydrate/high fat liquid diet. While we are currently unable to directly measure circulating FGF15 concentrations, *Fgf15* mRNA levels in ileum and downstream ERK1/2 phosphorylation in liver peaked approximately 1 hr post gavage. Similarly, serum FGF19 levels increase in humans 2–3 hr following a meal, when bile acid flux increases across the ileum (Lundasen, Galman et al. 2006). We believe that FGF15/19 is providing a mechanism to maintain glucose levels when circulating insulin levels drop, allowing for a smooth transition from the fasted to the fed state. The physiologic importance of this pathway is underscored by FGF15 KO and FGFR4 KO mice, which have increased gluconeogenic gene expression under fed conditions and hyperglycemia in response to fasting-refeeding challenge.

Moreover, FGF15 KO mice have elevated glucose levels in response to pyruvate/lactate challenge.

We also show that FGF15/19 inhibits gluconeogenic gene expression through a pathway distinct from insulin. Phosphorylation of CREB at Ser133, which occurs during fasting, causes it to associate with the CBP and p300 to induce gluconeogenic gene expression (Gonzalez and Montminy 1989; Chrivia, Kwok et al. 1993; Kwok, Lundblad et al. 1994). FGF15/19 causes the dephosphorylation of CREB and limits its recruitment to the *Pgc1α* and *G6Pase* promoters. Even though attempts were made to elucidate the mechanism, it is presently unclear how FGF15/19 signaling causes CREB dephosphorylation.

In summary, we show that FGF15/19 inhibits hepatic gluconeogenesis through a pathway involving inhibition of the CREB-PGC-1α signaling cascade. We conclude that FGF15/19 is a late postprandial signal in the temporal cascade of hormones that control hepatic metabolism in response to nutritional status.

3.4 Acknowledgments

I would like to acknowledge the important contributions that Dr. Matthew Potthoff made to this project. He began working on this project alone and allowed me to work alongside him in developing this story. He deserves full credit for the work involving the NMR tracer studies and the mircroarray analysis as I was not part of those initial experiments. We worked together on most every aspect of all

other experiments. I also want to thank Dr. Robert Gerard for preparing all of our adenoviruses; Drs. Kelly Suino-Powell and Eric Xu for the rFGF19 protein; Dr. Bruce Spiegelman for the PGC-1$\alpha^{fl/fl}$ mice; Dr. Marc Montminy for the Ad-CRE-luc adenovirus and p-CREB antibodies; Dr. Shawn Burgess and the members of his lab for the NMR tracer studies and GC-MS support; Drs. Yuan Zhang, Angie Bookout, Serkan Kir, and Xunshan Ding for technical assistance.

Chapter 4.

The Role of FGF21 Regulation in Hepatic Cell Signaling Cascades *in vitro* and *in vivo*

4.1 Introduction

FGF21 is a hormone that regulates glucose and lipid metabolism, physiologically and pharmacologically. During fasting, FGF21 is induced in the liver by fatty acids from the WAT acting through the nuclear receptor, PPARα (Badman, Pissios et al. 2007; Inagaki, Dutchak et al. 2007; Lundasen, Hunt et al. 2007). Recently, FGF21 was also found to be induced in WAT by the nuclear receptor, PPARγ, during feeding (Dutchak, Katafuchi et al. 2012). Pharmacologically, FGF21 improves glucose homeostasis, reduces adiposity, and improves lipid profiles in both diabetic rodents and rhesus monkeys (Kharitonenkov, Shiyanova et al. 2005; Kharitonenkov, Wroblewski et al. 2007; Coskun, Bina et al. 2008; Xu, Lloyd et al. 2009). However, the mechanisms that govern these potent insulin sensitizing effects of FGF21 have not been elucidated.

FetuinA, also known as Ahsg, is a phosphorylated glycoprotein synthesized and secreted by the liver. FetuinA interacts with activated insulin receptor (IR) to repress insulin-induced IR autophosphorylation and downstream signaling activity (Auberger, Falquerho et al. 1989; Srinivas, Wagner et al. 1993; Mathews, Chellam et al. 2000). This inhibitory activity of FetuinA is regulated by its phosphorylation status (Auberger, Falquerho et al. 1989). FetuinA KO mice demonstrate improved insulin sensitivity and resistance to high-fat diet (HFD) (Mathews, Singh et al. 2002; Mathews, Rakhade et al. 2006). Interestingly, the

gene for FetuinA is associated with an increased risk of type 2 diabetes (Kissebah, Sonnenberg et al. 2000).

In this chapter, I demonstrate that SILAC can be used to identify novel signaling targets of FGF21 in H4IIE cells, including FetuinA. I had hypothesized that FGF21 could be mediating its insulin sensitizing effects by dephosphorylating FetuinA. I developed a phospho-specific antibody to FetuinA to examine the effects of FGF21 on its regulation *in vivo*. Unfortunately, FGF21 does not play a role in the *in vivo* regulation of FetuinA or other identified targets. The results demonstrate that despite targets being regulated by FGF21 *in vitro* these results are not recapitulated *in vivo*.

4.2 Results

Although the advantageous metabolic effects of administering FGF21 have been extensively studied, the cellular events mediating these effects are not well understood. To understand the molecular mechanisms regulating the effects of FGF21, we began studying the downstream kinase signaling cascades and the protein substrates affected by this hormone. Utilizing stable isotope labeling of amino acids in cell culture (SILAC) followed by phosphopeptide enrichment, an unbiased phosphoproteomic profile was obtained of potential FGF21 targets in rat H4IIE hepatocyte cells (Fig. 4.1). A total of 52 unique phosphopeptides were identified as being regulated if greater than 1.5-fold change was observed with

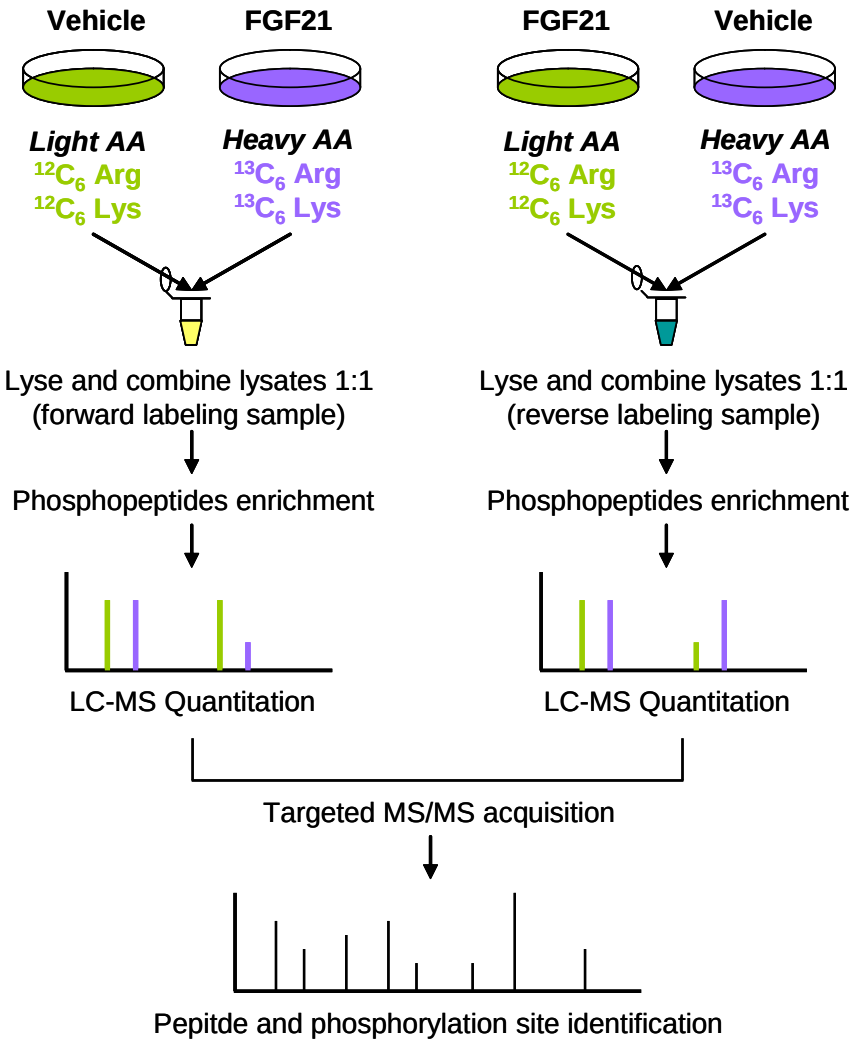

Figure 4.1: Schematic Representation of SILAC-MS Approach for Phosphopeptide Profiling

Stable isotope labeling with amino acids in cell culture (SILAC) is a quantitative mass spectrometry (MS)-based technique to identify differences in protein abundance between two samples. SILAC relies on metabolic incorporation of a given 'light' or 'heavy' form of the amino acid into the proteins. Lysates from cells grown in different conditions are compared by mixing the populations and enriching for phosphopeptides prior to LC-MS analysis. Relative peptide differences can be compared using the known mass shift of the labeled amino acids.

FGF21 treatment. Several targets had multiple phosphorylation sites associated with unique phosphopeptides, reducing the total number of target proteins to 46. As expected, ERK1/2, a known FGF21 signaling target, was identified. To validate the FGF21 responsive targets, a concentration curve of FGF21 treatment for was performed in H4IIE cells. Interestingly, PRAS40 phosphorylation increased gradually with increasing FGF21 concentration (Fig. 4.2). As expected, ERK1/2 phosphorylation showed a similar profile (Fig. 4.2). These data demonstrate the ability of a phosphoprofiling platform to identify novel FGF21 signaling targets.

Interestingly, one of the most highly regulated targets was FetuinA, which was dephosphorylated 6.2-fold by FGF21 treatment. FetuinA is an inhibitor of insulin receptor signaling and the FetuinA knockout mouse exhibits aberrant glucose homeostatsis (Auberger, Falquerho et al. 1989; Mathews, Singh et al. 2002). The similarities between the Fetuin-A KO mice and the FGF21tg mice are striking (Table 4.1), thus prompting investigation into the regulation of this protein. To assess whether FGF21 can alter FetuinA, H4IIE cells were treated with FGF21. Both FetuinA mRNA and protein levels were unchanged in the presence of FGF21 (Fig 4.3A &B). However, when phosphoproteins were isolated from vehicle or FGF21-treated H4IIE cells, a reduction in phosphorylated FetuinA was observed in the presence of FGF21 (Fig. 4.3C). Taken together,

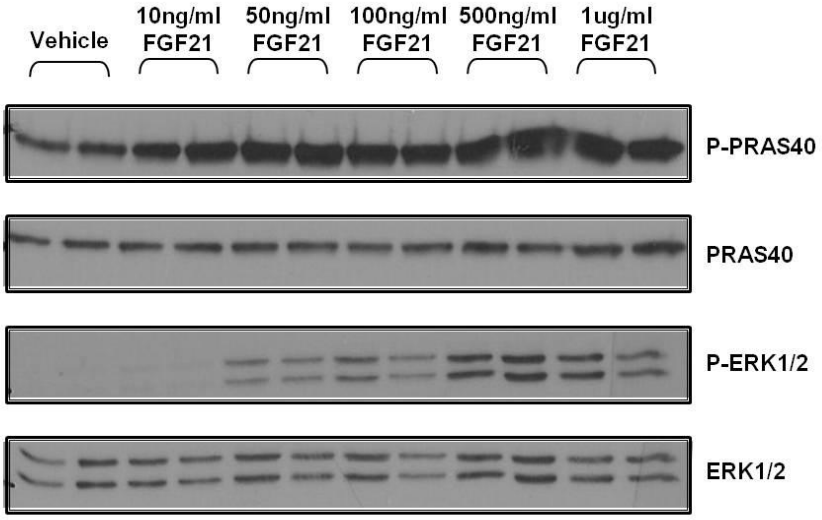

Figure 4.2: FGF21 Alters Phosphorylation Status of Proteins in H4IIE Cells
H4IIE cells were treated with vehicle or FGF21 for 10min. Lysates were prepared and subjected to Western blot analysis.

Table 4.1: FetuinA KO and FGF21tg Mouse Comparison Chart

	FetuinA KO	FGF21tg
Decreased Fasting FFAs and TGs	√	√
Enhanced Glucose Clearance	√	√
Increased Insulin Sensitivity	√	√
Increased Glucose Utilization	√	√
Resistant to DIO	√	√
Increased Energy Expenditure	√	√
Smaller in Size	√	√

Summary of the published metabolic phenotypes exhibited by the FetuinA KO and the FGF21tg mice.

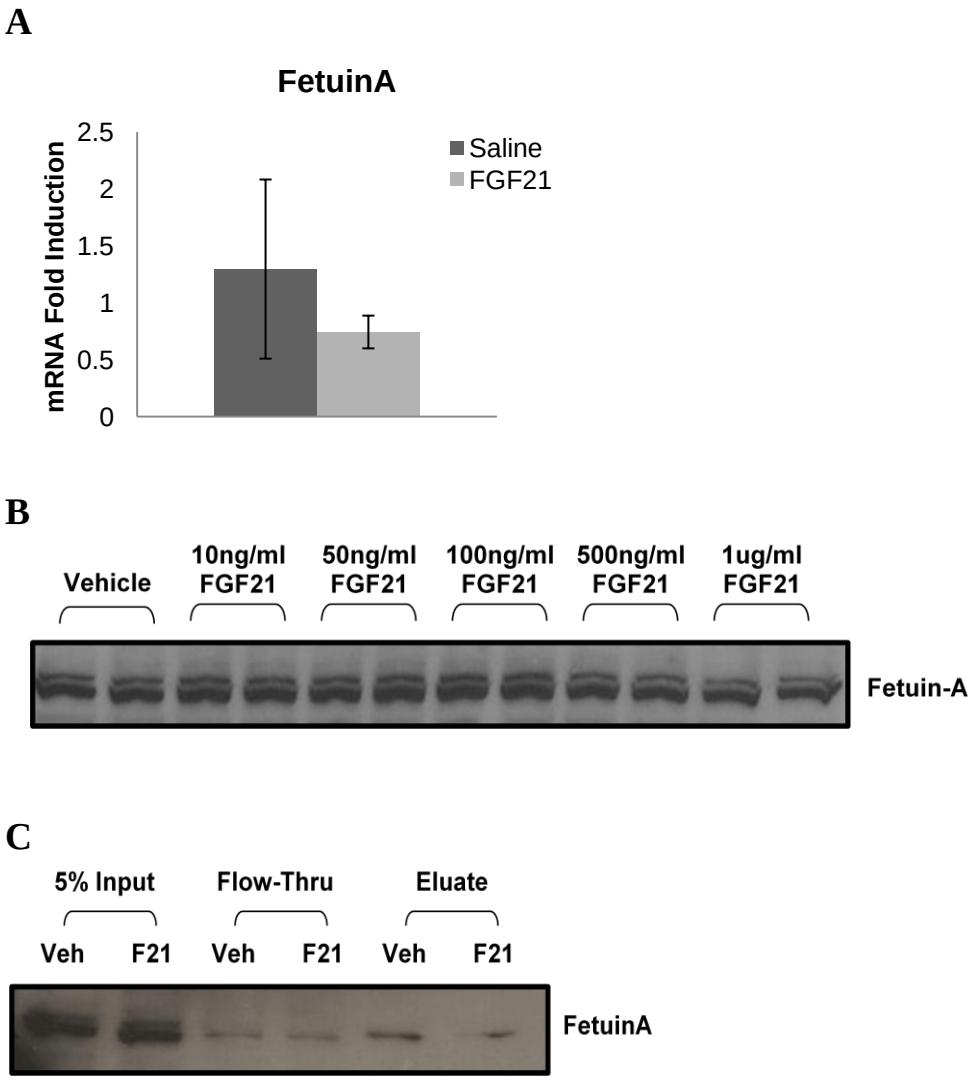

Figure 4.3: FGF21 Decreases the Phosphorylation Status of FetuinA in H4IIE Cells

H4IIE cells were treated with vehicle or 1.0ug/ml FGF2 for 10min unless otherwise stated. (A) mRNA was measured after 6h FGF21 treatment by qPCR. Data are represented as the mean ± SEM. (B) Lysates were prepared and subjected to Western blot analysis. (C) Phosphoprotein purifications were performed. Samples were prepared and subjected to Western blot analysis.

these data demonstrate that FGF21 does not regulate FetuinA at the transcriptional or translational level but decreases its phosphorylation status.

To determine whether Fetuin-A can mediate the pharmacological effects of FGF21, it became necessary to produce, purify, and validate a FetuinA phospho-specific antibody. Based on the phosphopeptides identified in the initial screening platform, immunizing peptides were designed for the three phosphorylated residues: serine 120 (Ser120), serine 309 (Ser309), and serine 314 (Ser314). While an adequate antibody was produced for phosphorylated FetuinA at Ser309, both the Ser120 and Ser314 attempts were unsuccessful (data not shown). After negative and positive affinity column purification, the Ser309-FetuinA antibody and resulting pan-FetuinA antibody were validated by verifying their ability to detect FetuinA in mouse plasma when compared to a commercially available total FetuinA antibody (Fig.4.4A). To confirm that the Ser309-FetuinA antibody was specific, we used both protein phosphatase treatment and peptide blocking. Pooled mouse plasma was treated with lambda protein phosphatase to eliminate all phosphorylated proteins. Samples treated with phosphatase were undetectable with the phospho-specific FetuinA antibody but not the total (Fig.4.4B). For peptide blocking, the corresponding peptide and the Ser309-FetuinA antibody were incubated together to quench its binding capacity for its

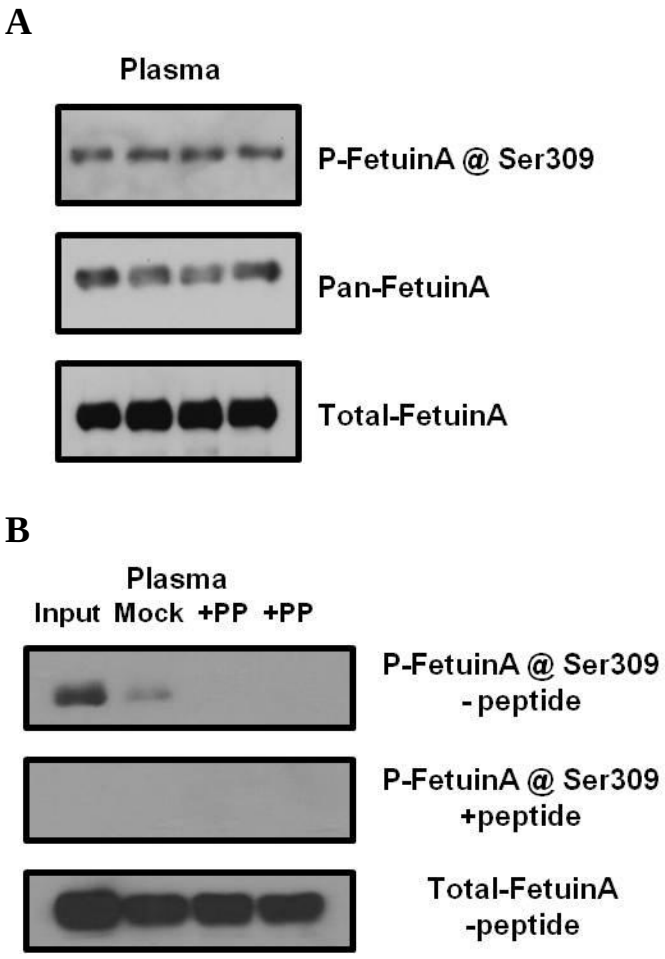

Figure 4.4: Validation of a Specific Serine 309 Phospho-FetuinA Antibody
Plasma was collected from WT mice. (A) Plasma was subjected to Western blot analysis. (B) Pooled plasma (n=4) was treated with either vehicle or protein phosphatase and subjected to a modified Western blot analysis with or without peptide blocking.

substrate. In the presence of the blocking peptide, all plasma samples were undetectable signifying a specificity for Fetuin-A, particularly when phosphorylated at Ser309 (Fig.4.4B). Taken together, these data show that we produced an antibody specific for FetuinA phosphorylated at Ser309.

To gain insight into whether FGF21 regulates FetuinA *in vivo*, we examined our FGF21tg and FGF21 KO mouse models. Gene expression of FetuinA was examined in FGF21tg, FGF21 KO, and their respective wildtype counterparts every 4 hours within a 24-hour period. The overexpression or absence of FGF21 had no effect on FetuinA mRNA levels (Fig. 4.5). Surprisingly, when Ser309-FetuinA levels were analyzed in the FGF21tg mice, no change was observed in either the liver (Fig 4.6A) or circulating plasma levels (Fig. 4.6B). These data led us to analyze other signaling cascades in the FGF21 KO and FGF21tg mice. We did not observe any differences in the phosphorylation of ERK1/2 or PRAS40 in the absence or overexpression of FGF21 (Fig 4.7). Taken together, these data suggested that signaling cascades are not disrupted in the FGF21tg or FGF21 KO mice.

To assess whether Fetuin-A could be playing a role in the insulin-sensitizing effects of FGF21, we used 16-week DIO mice and treated with either vehicle or FGF21. As expected, FGF21 caused a reduction in insulin and glucose levels (Fig.4.8A & B). While ERK1/2 phosphorylation was increased, the phosphorylation status of PRAS40 and FetuinA remained unchanged in the liver

A

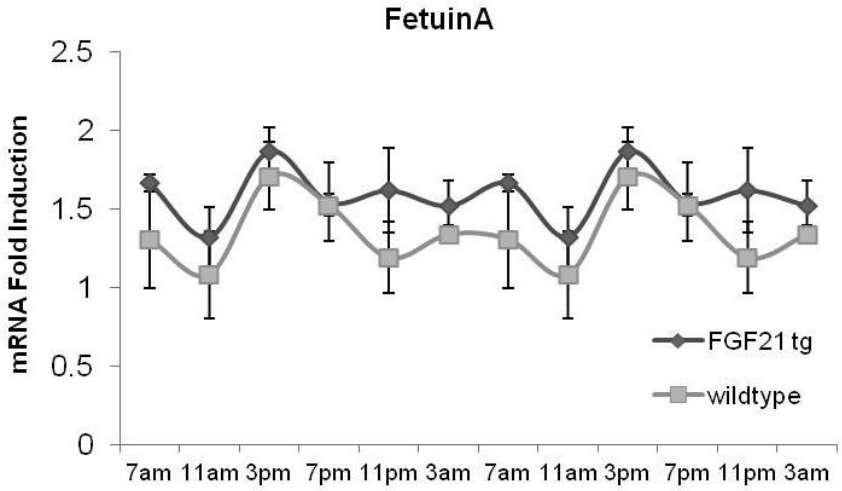

B

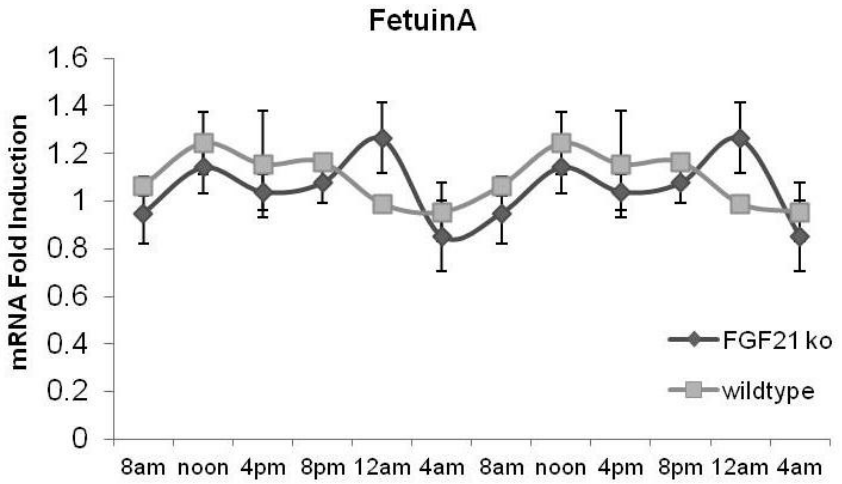

Figure 4.5: FGF21 Does Not Alter Hepatic FetuinA Gene Expression
Hepatic mRNA from (A) FGF21tg, (B) FGF21 KO mice and their WT counterparts were measured by qPCR from samples collected every 4h within a 24h period. Data are expressed as the fold change ± SEM.

A

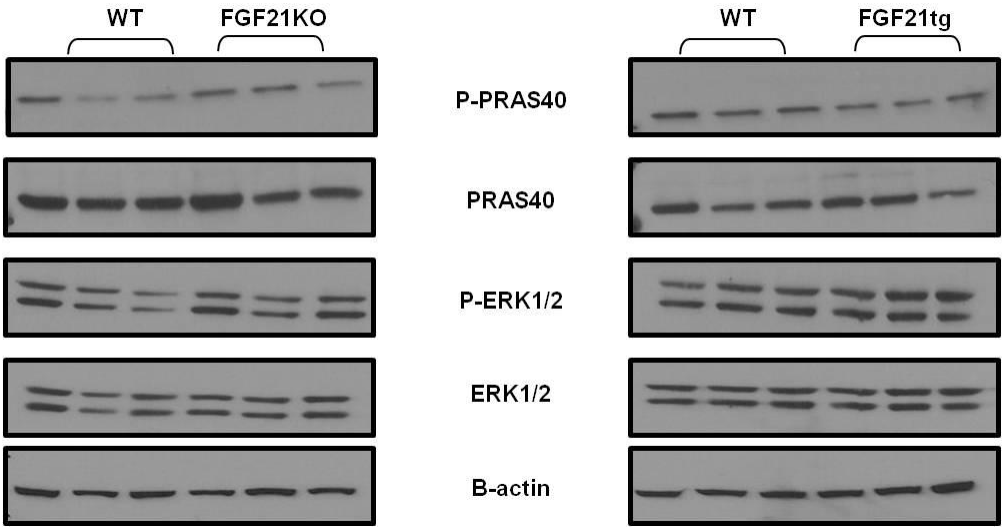

Figure 4.6: FGF21 Does Not Alter Hepatic Signaling Cascades
Liver lysates from (A) FGF21 KO, (B) FGF21tg and their WT counterparts were subjected to Western blot analysis.

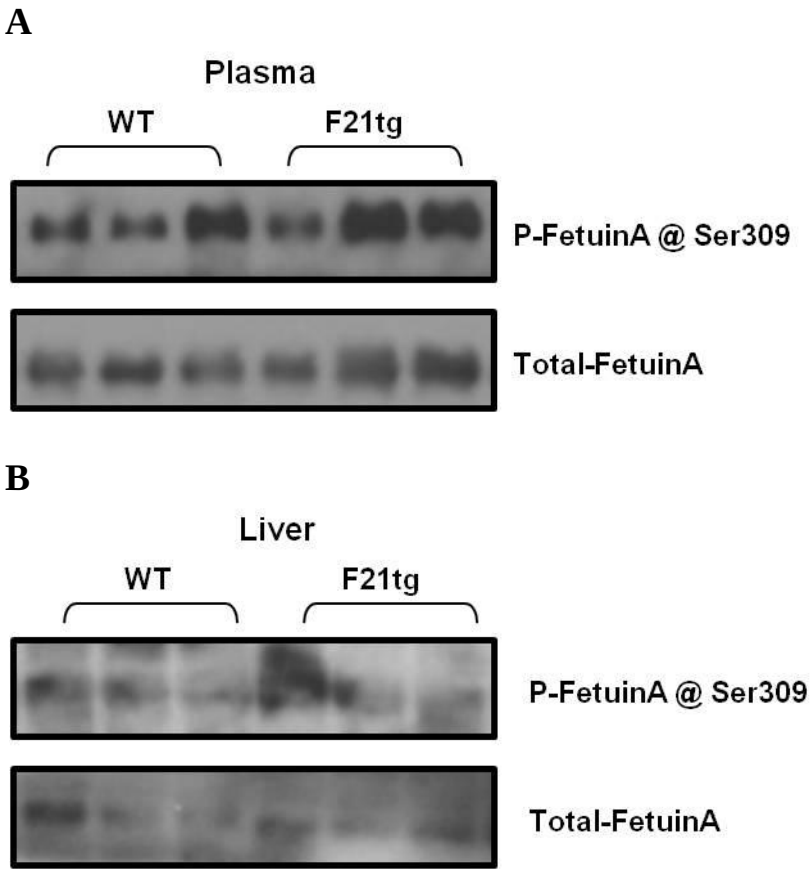

Figure 4.7: FGF21tg Mice Do Not Have Altered Levels of P-FetuinA
(A) Plasma and (B) liver lysates from WT and FGF21tg mice were subjected to Western blot analysis.

(Fig.4.8.C). Unfortunately, when circulating FetuinA levels were examined no difference was observed (Fig. 4.8.D). Sadly, these data imply that FGF21 is not utilizing the phosphorylation status of FetuinA as a mechanism to alter insulin sensitivity.

To determine the relevance of Fetuin-A in regulating signaling cascades, we went back to the H4IIE cells and performed a knockdown experiment of Fetuin-A. Using three different FetuinA-specific siRNAs, we were able to reduce Fetuin-A mRNA and protein levels roughly 60% (Fig4.9A & B). However, the absence of Fetuin-A in H4IIE cells did not alter their ability to respond to FGF21 and induce phosphorylation of ERK1/2 (Fig. 4.9B). These data suggest that Fetuin-A is dispensible for FGF21 to mediate its effects in H4IIE cells.

Taken together, the data suggest that perhaps FGF21 is not acting directly on the liver but through other tissues. To address this possibility, we utilized the total β-Klotho KO and liver-specific β-Klotho KO models. We treated the total β-Klotho KO, liver-specific β-Klotho KO, and their WT counterparts with FGF21 to examine hepatic signaling. As expected, the WT mice responded to FGF21 with an increase in ERK1/2 phosphorylation, but the total β-Klotho KO mice were unable to elicit a response (Fig4.10A). FGF21-induced ERK1/2 phosphorylation was also lost in the liver-specific β-Klotho KO mice (Fig4.10B). Taken together, these data show that FGF21 can signal directly to the liver to regulate hepatic signaling cascades.

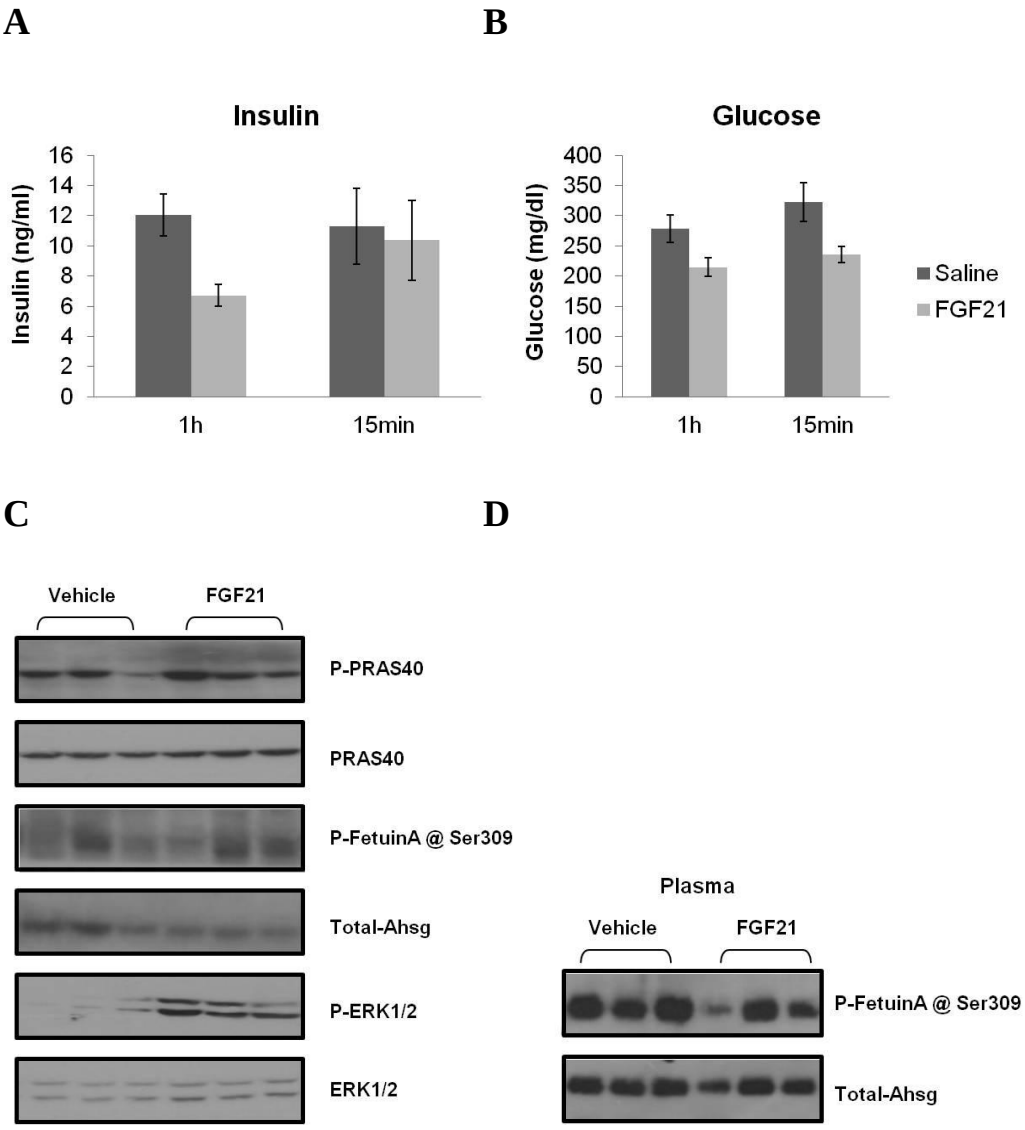

Figure 4.8: FGF21 Treatment Does Not Alter P-FetuinA Levels in DIO Mice
DIO mice were injected with either vehicle or 1.0mg/kg FGF21 for 15min or 1h. Plasma (A) insulin and (B) glucose levels were measured and represented as the mean ± SEM. (C) Liver lysates and (D) plasma from 1h treatment group were subjected to Western blot analysis.

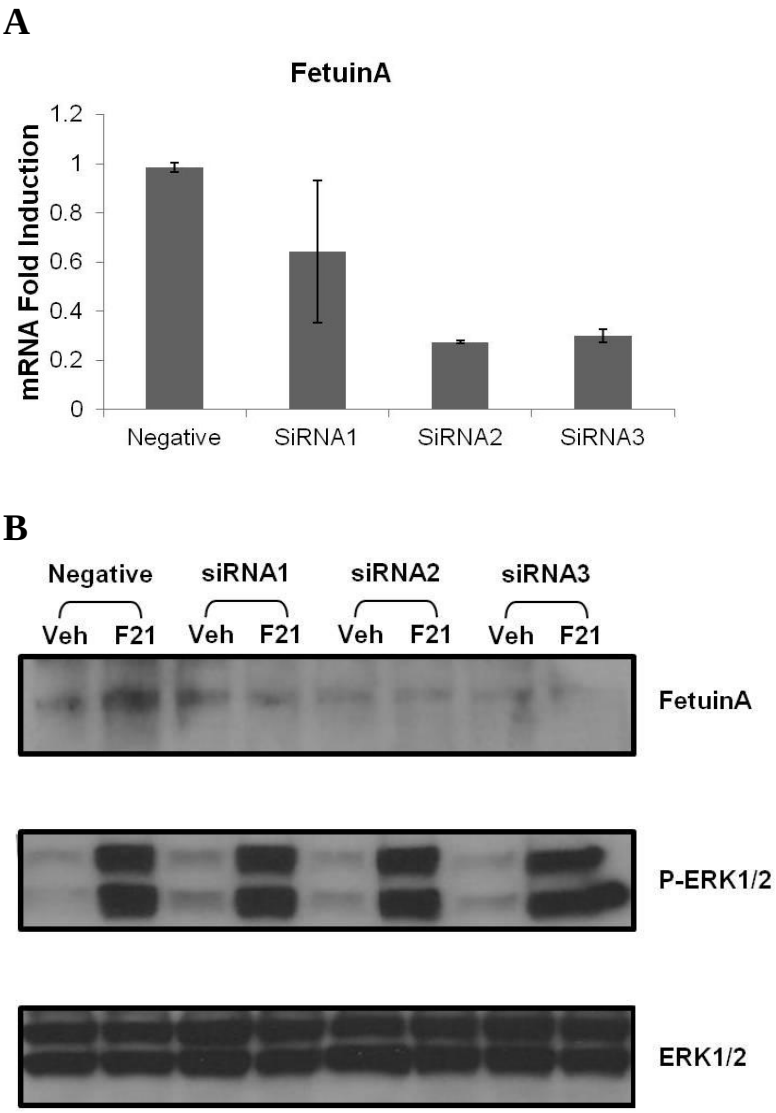

Figure 4.9: FGF21 Does Not Require FetuinA to Alter Signaling Cascades
H4IIE cells were transfected with either control or FetuinA-specific siRNA for 48h before treatment with vehicle or 1.0ug/ml FGF21 for 10min. (A) mRNA was measured by qPCR. Data are represented as the mean ± SEM. (B) Lysates were prepared and subjected to Western blot analysis.

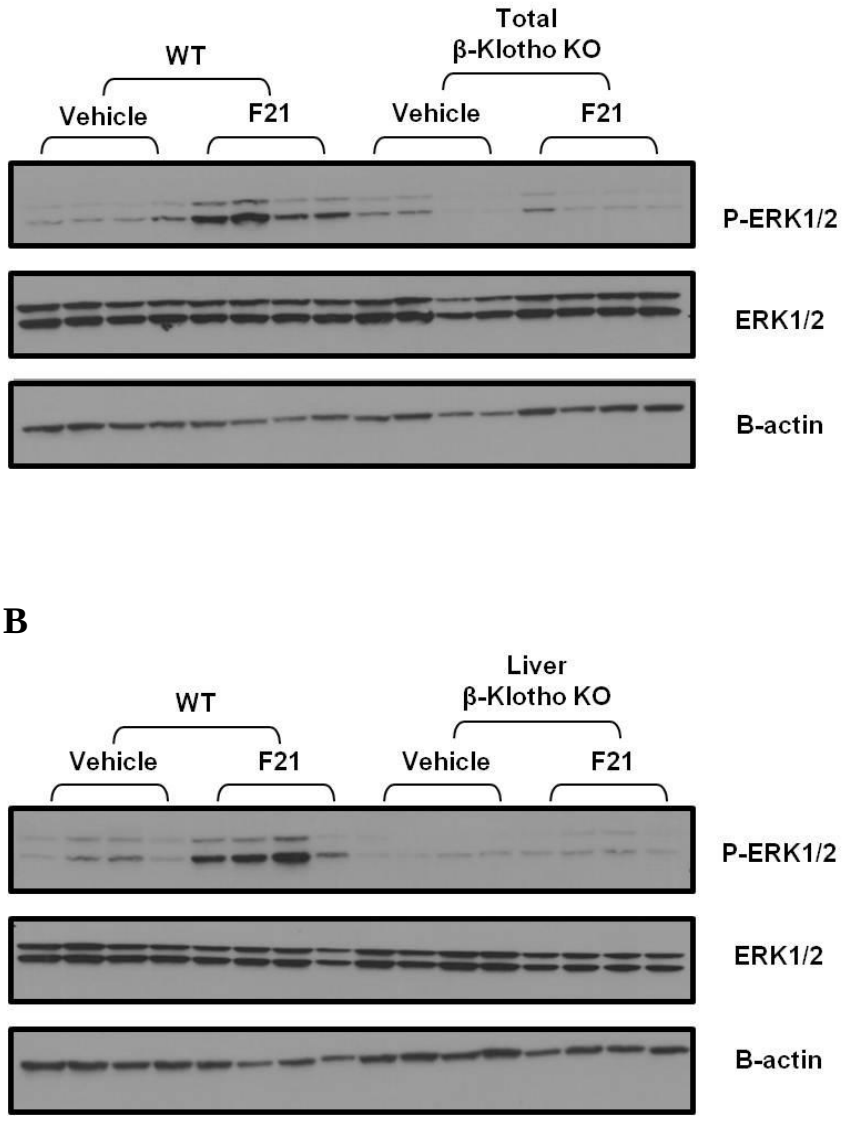

Figure 4.10: FGF21 Requires Hepatic β-Klotho to Induce Signaling in the Liver

B-Klotho (A) Total KO, (B) Liver-Specific KO and their WT counterparts were treated with either vehicle or 1.0mg/kg of FGF21 for 1h. Liver lysates were subjected to Western blot analysis.

4.3 Discussion

In these experiments, we show an unbiased phosphoproteomic platform in H4IIE cells can identify novel FGF21 targets. The most highly regulated target was FetuinA, which was dephosphorylated by FGF21 treatment. Excitingly, FetuinA is an insulin receptor inhibitor but only when phosphorylated (Auberger, Falquerho et al. 1989). FetuinA interacts with insulin receptor to repress its autophosphorylation and downstream signaling activity (Auberger, Falquerho et al. 1989; Mathews, Chellam et al. 2000). Upon closer examination, we discovered that the identified phosphopeptides within FetuinA were found in circulating human plasma (Haglund, Ek et al. 2001). Interestingly, the FetuinA KO mice exhibit enhanced glucose clearance, increased insulin sensitivity, resistance to diet-induced obesity, and increased energy expenditure (Mathews, Singh et al. 2002; Mathews, Rakhade et al. 2006). The striking similarities between the FetuinA KO and FGF21tg mouse led us to hypothesize that FGF21 could be regulating FetuinA. We proposed that FGF21 was causing a decrease in FetuinA phosphorylation that led to its inability to inhibit the insulin receptor, thereby enhancing insulin signaling. The derepression of the system would allow for an immediate response to enhance insulin sensitivity. Despite the convincing evidence from the literature and in H4IIE cells, we were unable to find a relationship between FGF21 and FetuinA. Unfortunately, the novel targets identified using SILAC and phosphoprotein enrichment in H4IIE cells could not

be translated to a mouse model. The results call into question the use of cell-based systems to analyze the mechanisms and effects of compounds as a surrogate for animal models. However, the simplicity and conformity of these systems cannot be denied and should be used when possible.

We also show that FGF21 requires hepatic β-Klotho to elicit a signaling response in the liver. These experiments were motivated by the inability to translate the protein targets identified with SILAC into an *in vivo* model. Due to β-Klotho expression within the CNS (Fon Tacer, Bookout et al. 2010), it seemed possible that FGF21 could be indirectly affecting hepatic signaling pathways. However, our results indicate that FGF21 acts directly on the liver to alter phosphorylation cascades. The basis for the differences between cell culture and mouse models remains unclear.

In summary, we show that FetuinA phosphorylation is inhibited by FGF21 in H4IIE cells, but is not altered in a mouse model. We conclude that FGF21 is not mediating its insulin-sensitizing effects through the regulation of FetuinA phoshphorylation status.

4.4 Acknowledgments

I am very grateful to the Merck Research Laboratories for performing the technically challenging SILAC profiling studies. I also want to extend my deepest thanks to Ewa Borowiz for her contributions in the development of the P-FetuinA

antibodies and her technical assistance; Drs. Regina Goetz and Moosa Mohammadi for the rFGF21 protein; Dr. Angie Bookout for the circadian rhythm samples and technical assistance; Dr. Xunshan Ding for access to the β-Klotho KO mice and technical assistance. I also want to thank Dr. Yuan Zhang, Heather Lawerence, Dr. Matthew Potthoff, and Dr. Bryn Owen for technical assistance.

Chapter 5.

Concluding Remarks & Perspectives

The theme of my dissertation has been to understand the molecular mechanisms that FGF15/19 and FGF21 use to mediate effects on glucose homeostasis. In the case of FGF15/19, we found it acts in a very similar fashion to insulin but utilizes different cellular signal transduction pathways. The potential use of FGF15/19 in successfully treating insulin insensitivity and type 2 diabetes could be significant. Previously, hesitation for its use arose due to its proliferative capabilities and potential cancer promoting properties. However, the experiments showing that the FGF15/19 polypeptide can be re-engineered to maintain only its metabolic effects have given new hope to the field (Wu, Ge et al. 2009).

One caveat to our studies has been the inability to detect FGF15 in circulation. While tools exist to measure FGF19, it has been technically challenging to develop FGF15 antibodies. We are currently working with several groups in the development of an antibody that can be used. We hope to gain insight into the timing and location of its release. We expect to see increased serum FGF15 levels 1-2 hr following refeeding based on our mRNA studies. As serum FGF19 levels are increased in humans 2–3 hr following a meal (Lundasen, Galman et al. 2006), this seems highly probable. However, several possibilities exist for its distribution when released into circulation. FGF15 could quickly be degraded or its release could be restricted to the hepatic portal tract limiting its effects to the gastrointestinal system. This seems likely, as the glucose

homeostatic effects are much more dramatic when exogenous FGF19 is administered.

There is also the possibility that the liver is not the only tissue through which FGF19 can function. Evidence exists that it acts on the WAT, but what about the CNS? The inability to recapitulate our findings in cell culture or primary hepatocytes suggests a more complicated mechanism. The development of the tissue-specific β-Klotho KO mice now gives us the ability to determine whether all or some of its affects are due to the liver or other tissues.

Unfortunately, the FGF21 results leave unanswered questions. We still do not understand the molecular underpinnings of its insulin sensitizing effects. The reasons for the inability to translate the in vitro results into the mouse remain unclear. However, current work in our lab suggests that FGF21 is mediating most its effects through the hypothalamus and not through the liver. If liver is not a direct target of FGF21, the results from the phosphoprofiling platform could be misleading. I believe that this could account for the differences seen in the mouse liver and H4IIE cells, although the results utilizing the liver-specific β-Klotho KO would suggest that FGF21 can directly signal to the liver. Unfortunately, unpublished data from our laboratory suggests the liver is not the site of the insulin sensitizing effects. The results from my experiments could be an artifact of the pharmacological doses given to the mice but with no functional relevance. Again, the development of the tissue-specific β-Klotho KO mice gives us the

ability to identify which tissues FGF21 acts to mediate its effects. However, once we determine the relevant tissues I would approach the question in a similar manner. I believe the phosphoprotein isolation coupled with SILAC is still a very powerful tool in helping us to elucidate signaling pathways in an unbiased manner.

In my four years as a graduate student in the Mango/Kliewer lab, I have helped to establish the role of FGF15/19 in glucose homeostatsis and have provided evidence that FGF21 is not eliciting its insulin sensitizing effects through the liver. It is my hope that my work will help provide insight for the future work in the laboratory for their continued success.

Bibliography

Ahren, B. and P. J. Havel (1999). "Leptin increases circulating glucose, insulin and glucagon via sympathetic neural activation in fasted mice." Int J Obes Relat Metab Disord **23**(6): 660-665.

Auberger, P., L. Falquerho, et al. (1989). "Characterization of a natural inhibitor of the insulin receptor tyrosine kinase: cDNA cloning, purification, and anti-mitogenic activity." Cell **58**(4): 631-640.

Badman, M. K., P. Pissios, et al. (2007). "Hepatic fibroblast growth factor 21 is regulated by PPARalpha and is a key mediator of hepatic lipid metabolism in ketotic states." Cell Metab **5**(6): 426-437.

Beenken, A. and M. Mohammadi (2009). "The FGF family: biology, pathophysiology and therapy." Nat Rev Drug Discov **8**(3): 235-253.

Berglund, E. D., C. Y. Li, et al. (2009). "Fibroblast growth factor 21 controls glycemia via regulation of hepatic glucose flux and insulin sensitivity." Endocrinology **150**(9): 4084-4093.

Bookout, A. L., Y. Jeong, et al. (2006). "Anatomical profiling of nuclear receptor expression reveals a hierarchical transcriptional network." Cell **126**(4): 789-799.

Burgess, S. C., T. C. Leone, et al. (2006). "Diminished hepatic gluconeogenesis via defects in tricarboxylic acid cycle flux in peroxisome proliferator-activated

receptor gamma coactivator-1alpha (PGC-1alpha)-deficient mice." J Biol Chem **281**(28): 19000-19008.

Burgess, S. C., B. Weis, et al. (2003). "Noninvasive evaluation of liver metabolism by 2H and 13C NMR isotopomer analysis of human urine." Anal Biochem **312**(2): 228-234.

Choi, M., A. Moschetta, et al. (2006). "Identification of a hormonal basis for gallbladder filling." Nat Med **12**(11): 1253-1255.

Chrivia, J. C., R. P. Kwok, et al. (1993). "Phosphorylated CREB binds specifically to the nuclear protein CBP." Nature **365**(6449): 855-859.

Coskun, T., H. A. Bina, et al. (2008). "Fibroblast growth factor 21 corrects obesity in mice." Endocrinology **149**(12): 6018-6027.

Dalle, S., C. Longuet, et al. (2004). "Glucagon promotes cAMP-response element-binding protein phosphorylation via activation of ERK1/2 in MIN6 cell line and isolated islets of Langerhans." J Biol Chem **279**(19): 20345-20355.

Dentin, R., Y. Liu, et al. (2007). "Insulin modulates gluconeogenesis by inhibition of the coactivator TORC2." Nature **449**(7160): 366-369.

Dutchak, P. A., T. Katafuchi, et al. (2012). "Fibroblast growth factor-21 regulates PPARgamma activity and the antidiabetic actions of thiazolidinediones." Cell **148**(3): 556-567.

Evans, R. M., G. D. Barish, et al. (2004). "PPARs and the complex journey to obesity." Nat Med **10**(4): 355-361.

Finck, B. N. and D. P. Kelly (2006). "PGC-1 coactivators: inducible regulators of energy metabolism in health and disease." J Clin Invest **116**(3): 615-622.

Folch, J., M. Lees, et al. (1957). "A simple method for the isolation and purification of total lipides from animal tissues." J Biol Chem **226**(1): 497-509.

Fon Tacer, K., A. L. Bookout, et al. (2010). "Research resource: Comprehensive expression atlas of the fibroblast growth factor system in adult mouse." Mol Endocrinol **24**(10): 2050-2064.

Fu, L., L. M. John, et al. (2004). "Fibroblast growth factor 19 increases metabolic rate and reverses dietary and leptin-deficient diabetes." Endocrinology **145**(6): 2594-2603.

Gimeno, L., P. Brulet, et al. (2003). "Study of Fgf15 gene expression in developing mouse brain." Gene Expr Patterns **3**(4): 473-481.

Goetz, R., A. Beenken, et al. (2007). "Molecular insights into the klotho-dependent, endocrine mode of action of fibroblast growth factor 19 subfamily members." Mol Cell Biol **27**(9): 3417-3428.

Goldfarb, M. (2005). "Fibroblast growth factor homologous factors: evolution, structure, and function." Cytokine Growth Factor Rev **16**(2): 215-220.

Gonzalez, G. A. and M. R. Montminy (1989). "Cyclic AMP stimulates somatostatin gene transcription by phosphorylation of CREB at serine 133." Cell **59**(4): 675-680.

Goodwin, B., S. A. Jones, et al. (2000). "A regulatory cascade of the nuclear receptors FXR, SHP-1, and LRH-1 represses bile acid biosynthesis." Mol Cell **6**(3): 517-526.

Hagiwara, M., A. Alberts, et al. (1992). "Transcriptional attenuation following cAMP induction requires PP-1-mediated dephosphorylation of CREB." Cell **70**(1): 105-113.

Haglund, A. C., B. Ek, et al. (2001). "Phosphorylation of human plasma alpha2-Heremans-Schmid glycoprotein (human fetuin) in vivo." Biochem J **357**(Pt 2): 437-445.

Handschin, C. and B. M. Spiegelman (2006). "Peroxisome proliferator-activated receptor gamma coactivator 1 coactivators, energy homeostasis, and metabolism." Endocr Rev **27**(7): 728-735.

Hashimoto, T., W. S. Cook, et al. (2000). "Defect in peroxisome proliferator-activated receptor alpha-inducible fatty acid oxidation determines the severity of hepatic steatosis in response to fasting." J Biol Chem **275**(37): 28918-28928.

Herzig, S., S. Hedrick, et al. (2003). "CREB controls hepatic lipid metabolism through nuclear hormone receptor PPAR-gamma." Nature **426**(6963): 190-193.

Herzig, S., F. Long, et al. (2001). "CREB regulates hepatic gluconeogenesis through the coactivator PGC-1." Nature **413**(6852): 179-183.

Hogg, R. T., J. A. Garcia, et al. (2010). "Adenoviral targeting of gene expression to tumors." Cancer Gene Ther **17**(6): 375-386.

Holt, J. A., G. Luo, et al. (2003). "Definition of a novel growth factor-dependent signal cascade for the suppression of bile acid biosynthesis." Genes Dev **17**(13): 1581-1591.

Inagaki, T., M. Choi, et al. (2005). "Fibroblast growth factor 15 functions as an enterohepatic signal to regulate bile acid homeostasis." Cell Metab **2**(4): 217-225.

Inagaki, T., P. Dutchak, et al. (2007). "Endocrine regulation of the fasting response by PPARalpha-mediated induction of fibroblast growth factor 21." Cell Metab **5**(6): 415-425.

Inagaki, T., V. Y. Lin, et al. (2008). "Inhibition of growth hormone signaling by the fasting-induced hormone FGF21." Cell Metab **8**(1): 77-83.

Ito, S., T. Fujimori, et al. (2005). "Impaired negative feedback suppression of bile acid synthesis in mice lacking betaKlotho." J Clin Invest **115**(8): 2202-2208.

Itoh, N. (2007). "The Fgf families in humans, mice, and zebrafish: their evolutional processes and roles in development, metabolism, and disease." Biol Pharm Bull **30**(10): 1819-1825.

Itoh, N. and D. M. Ornitz (2004). "Evolution of the Fgf and Fgfr gene families." Trends Genet **20**(11): 563-569.

Itoh, N. and D. M. Ornitz (2008). "Functional evolutionary history of the mouse Fgf gene family." Dev Dyn **237**(1): 18-27.

Kalaany, N. Y. and D. J. Mangelsdorf (2006). "LXRS and FXR: the yin and yang of cholesterol and fat metabolism." Annu Rev Physiol **68**: 159-191.

Katoh, M. (2003). "Evolutionary conservation of CCND1-ORAOV1-FGF19-FGF4 locus from zebrafish to human." Int J Mol Med **12**(1): 45-50.

Kerr, T. A., S. Saeki, et al. (2002). "Loss of nuclear receptor SHP impairs but does not eliminate negative feedback regulation of bile acid synthesis." Dev Cell **2**(6): 713-720.

Kersten, S., J. Seydoux, et al. (1999). "Peroxisome proliferator-activated receptor alpha mediates the adaptive response to fasting." J Clin Invest **103**(11): 1489-1498.

Kharitonenkov, A., J. D. Dunbar, et al. (2008). "FGF-21/FGF-21 receptor interaction and activation is determined by betaKlotho." J Cell Physiol **215**(1): 1-7.

Kharitonenkov, A., T. L. Shiyanova, et al. (2005). "FGF-21 as a novel metabolic regulator." J Clin Invest **115**(6): 1627-1635.

Kharitonenkov, A., V. J. Wroblewski, et al. (2007). "The metabolic state of diabetic monkeys is regulated by fibroblast growth factor-21." Endocrinology **148**(2): 774-781.

Kir, S., S. A. Beddow, et al. (2011). "FGF19 as a postprandial, insulin-independent activator of hepatic protein and glycogen synthesis." Science **331**(6024): 1621-1624.

Kissebah, A. H., G. E. Sonnenberg, et al. (2000). "Quantitative trait loci on chromosomes 3 and 17 influence phenotypes of the metabolic syndrome." Proc Natl Acad Sci U S A **97**(26): 14478-14483.

Kurosu, H., M. Choi, et al. (2007). "Tissue-specific expression of betaKlotho and fibroblast growth factor (FGF) receptor isoforms determines metabolic activity of FGF19 and FGF21." J Biol Chem **282**(37): 26687-26695.

Kurosu, H. and O. M. Kuro (2009). "The Klotho gene family as a regulator of endocrine fibroblast growth factors." Mol Cell Endocrinol **299**(1): 72-78.

Kurosu, H., Y. Ogawa, et al. (2006). "Regulation of fibroblast growth factor-23 signaling by klotho." J Biol Chem **281**(10): 6120-6123.

Kwok, R. P., J. R. Lundblad, et al. (1994). "Nuclear protein CBP is a coactivator for the transcription factor CREB." Nature **370**(6486): 223-226.

Larsson, T., R. Marsell, et al. (2004). "Transgenic mice expressing fibroblast growth factor 23 under the control of the alpha1(I) collagen promoter exhibit

growth retardation, osteomalacia, and disturbed phosphate homeostasis." Endocrinology **145**(7): 3087-3094.

Leone, T. C., C. J. Weinheimer, et al. (1999). "A critical role for the peroxisome proliferator-activated receptor alpha (PPARalpha) in the cellular fasting response: the PPARalpha-null mouse as a model of fatty acid oxidation disorders." Proc Natl Acad Sci U S A **96**(13): 7473-7478.

Lin, J., P. H. Wu, et al. (2004). "Defects in adaptive energy metabolism with CNS-linked hyperactivity in PGC-1alpha null mice." Cell **119**(1): 121-135.

Lu, T. T., M. Makishima, et al. (2000). "Molecular basis for feedback regulation of bile acid synthesis by nuclear receptors." Mol Cell **6**(3): 507-515.

Lundasen, T., C. Galman, et al. (2006). "Circulating intestinal fibroblast growth factor 19 has a pronounced diurnal variation and modulates hepatic bile acid synthesis in man." J Intern Med **260**(6): 530-536.

Lundasen, T., M. C. Hunt, et al. (2007). "PPARalpha is a key regulator of hepatic FGF21." Biochem Biophys Res Commun **360**(2): 437-440.

Mangelsdorf, D. J., C. Thummel, et al. (1995). "The nuclear receptor superfamily: the second decade." Cell **83**(6): 835-839.

Mathews, S. T., N. Chellam, et al. (2000). "Alpha2-HSG, a specific inhibitor of insulin receptor autophosphorylation, interacts with the insulin receptor." Mol Cell Endocrinol **164**(1-2): 87-98.

Mathews, S. T., S. Rakhade, et al. (2006). "Fetuin-null mice are protected against obesity and insulin resistance associated with aging." Biochem Biophys Res Commun **350**(2): 437-443.

Mathews, S. T., G. P. Singh, et al. (2002). "Improved insulin sensitivity and resistance to weight gain in mice null for the Ahsg gene." Diabetes **51**(8): 2450-2458.

Mayr, B. and M. Montminy (2001). "Transcriptional regulation by the phosphorylation-dependent factor CREB." Nat Rev Mol Cell Biol **2**(8): 599-609.

McWhirter, J. R., M. Goulding, et al. (1997). "A novel fibroblast growth factor gene expressed in the developing nervous system is a downstream target of the chimeric homeodomain oncoprotein E2A-Pbx1." Development **124**(17): 3221-3232.

Mohammadi, M., S. K. Olsen, et al. (2005). "Structural basis for fibroblast growth factor receptor activation." Cytokine Growth Factor Rev **16**(2): 107-137.

Moore, D. D. (2007). "Physiology. Sister act." Science **316**(5830): 1436-1438.

Nicholes, K., S. Guillet, et al. (2002). "A mouse model of hepatocellular carcinoma: ectopic expression of fibroblast growth factor 19 in skeletal muscle of transgenic mice." Am J Pathol **160**(6): 2295-2307.

Nishimura, T., Y. Nakatake, et al. (2000). "Identification of a novel FGF, FGF-21, preferentially expressed in the liver." Biochim Biophys Acta **1492**(1): 203-206.

Nishimura, T., Y. Utsunomiya, et al. (1999). "Structure and expression of a novel human FGF, FGF-19, expressed in the fetal brain." Biochim Biophys Acta **1444**(1): 148-151.

Ogawa, Y., H. Kurosu, et al. (2007). "BetaKlotho is required for metabolic activity of fibroblast growth factor 21." Proc Natl Acad Sci U S A **104**(18): 7432-7437.

Ornitz, D. M. (2000). "FGFs, heparan sulfate and FGFRs: complex interactions essential for development." Bioessays **22**(2): 108-112.

Parker, J. C., K. M. Andrews, et al. (2002). "Glycemic control in mice with targeted disruption of the glucagon receptor gene." Biochem Biophys Res Commun **290**(2): 839-843.

Potthoff, M. J., T. Inagaki, et al. (2009). "FGF21 induces PGC-1alpha and regulates carbohydrate and fatty acid metabolism during the adaptive starvation response." Proc Natl Acad Sci U S A **106**(26): 10853-10858.

Puigserver, P. and B. M. Spiegelman (2003). "Peroxisome proliferator-activated receptor-gamma coactivator 1 alpha (PGC-1 alpha): transcriptional coactivator and metabolic regulator." Endocr Rev **24**(1): 78-90.

Russell, D. W. and K. D. Setchell (1992). "Bile acid biosynthesis." Biochemistry **31**(20): 4737-4749.

Saito, H., K. Kusano, et al. (2003). "Human fibroblast growth factor-23 mutants suppress Na+-dependent phosphate co-transport activity and 1alpha,25-dihydroxyvitamin D3 production." J Biol Chem **278**(4): 2206-2211.

Srinivas, P. R., A. S. Wagner, et al. (1993). "Serum alpha 2-HS-glycoprotein is an inhibitor of the human insulin receptor at the tyrosine kinase level." Mol Endocrinol **7**(11): 1445-1455.

Sunny, N. E. and B. J. Bequette (2010). "Gluconeogenesis differs in developing chick embryos derived from small compared with typical size broiler breeder eggs." J Anim Sci **88**(3): 912-921.

Suzuki, M., Y. Uehara, et al. (2008). "betaKlotho is required for fibroblast growth factor (FGF) 21 signaling through FGF receptor (FGFR) 1c and FGFR3c." Mol Endocrinol **22**(4): 1006-1014.

Tomiyama, K., R. Maeda, et al. (2010). "Relevant use of Klotho in FGF19 subfamily signaling system in vivo." Proc Natl Acad Sci U S A **107**(4): 1666-1671.

Tomlinson, E., L. Fu, et al. (2002). "Transgenic mice expressing human fibroblast growth factor-19 display increased metabolic rate and decreased adiposity." Endocrinology **143**(5): 1741-1747.

Wadzinski, B. E., W. H. Wheat, et al. (1993). "Nuclear protein phosphatase 2A dephosphorylates protein kinase A-phosphorylated CREB and regulates CREB transcriptional stimulation." Mol Cell Biol **13**(5): 2822-2834.

Wang, L., Y. K. Lee, et al. (2002). "Redundant pathways for negative feedback regulation of bile acid production." Dev Cell **2**(6): 721-731.

Wang, Y., L. Vera, et al. (2009). "The CREB coactivator CRTC2 links hepatic ER stress and fasting gluconeogenesis." Nature **460**(7254): 534-537.

Wei, W., P. A. Dutchak, et al. (2012). "Fibroblast growth factor 21 promotes bone loss by potentiating the effects of peroxisome proliferator-activated receptor gamma." Proc Natl Acad Sci U S A **109**(8): 3143-3148.

Wu, X., H. Ge, et al. (2010). "Separating mitogenic and metabolic activities of fibroblast growth factor 19 (FGF19)." Proc Natl Acad Sci U S A **107**(32): 14158-14163.

Wu, X., H. Ge, et al. (2009). "Selective activation of FGFR4 by an FGF19 variant does not improve glucose metabolism in ob/ob mice." Proc Natl Acad Sci U S A **106**(34): 14379-14384.

Xu, J., D. J. Lloyd, et al. (2009). "Fibroblast growth factor 21 reverses hepatic steatosis, increases energy expenditure, and improves insulin sensitivity in diet-induced obese mice." Diabetes **58**(1): 250-259.

Yu, C., F. Wang, et al. (2000). "Elevated cholesterol metabolism and bile acid synthesis in mice lacking membrane tyrosine kinase receptor FGFR4." J Biol Chem **275**(20): 15482-15489.